RGNZ/MGPB

Reservoir Quality Evaluation: Unveiling Diagenetic Transformations through Mineralogical and Petrophysical Analyses of the Upper Miocene Lacustrine Sandstones in the Pannonian Basin System, Croatia

Rudarsko-geološko-naftni zbornik
(The Mining-Geology-Petroleum Engineering Bulletin)
UDC: 552.5
DOI: 10.17794/rgn.2024.3.12

Original scientific paper

Mario Matošević[1]; Nenad Tomašić[2]; Adaleta Perković[3]; Štefica Kampić[4]; Marijan Kovačić[5]; Davor Pavelić[6]

[1] INA – Industrija nafte d.d., Exploration & Production, Field Development, Exploration & Production Laboratory, Lovinčićeva 4, 10000 Zagreb, Croatia, https://orcid.org/0000-0001-5220-2200

[2] University of Zagreb, Faculty of Science, Department of Geology, Division of Mineralogy & Petrology, Horvatovac 95, 10000 Zagreb, Croatia, https://orcid.org/0009-0006-1002-1587

[3] INA – Industrija nafte d.d., Exploration & Production, Field Development, Exploration & Production Laboratory, Lovinčićeva 4, 10000 Zagreb, Croatia,

[4] University of Zagreb, Faculty of Science, Department of Geology, Division of Mineralogy & Petrology, Horvatovac 95, 10000 Zagreb, Croatia, https://orcid.org/0000-0002-3555-9504

[5] University of Zagreb, Faculty of Science, Department of Geology, Division of Mineralogy & Petrology, Horvatovac 95, 10000 Zagreb, Croatia, https://orcid.org/0000-0001-6761-9260

[6] University of Zagreb, Faculty of Mining, Geology and Petroleum Engineering, Pierottijeva 6, 10000 Zagreb, Croatia, https://orcid.org/0000-0003-2697-448X

Abstract

The Upper Miocene lacustrine sandstones of the North Croatian Basin, located in the southwestern Pannonian Basin System, represent significant reservoirs for hydrocarbon exploration, yet their diagenetic evolution remains poorly understood. This study offers a comprehensive investigation into the diagenesis of these sandstones, analyzing samples from 14 exploration wells in the Sava and Drava depressions. Using petrographic analyses, scanning electron microscopy with energy-dispersive X-ray spectroscopy (SEM-EDS), X-ray diffraction (XRD), and petrophysical measurements, we aimed to explain the diagenetic processes affecting reservoir quality and hydrocarbon productivity. Our results reveal a consistent grain size distribution, modal composition, and diagenetic alterations across both depressions. Compaction, evidenced by evolving grain contacts and pressure dissolution, leads to a depth-dependent reduction in porosity. Carbonate cements, notably calcite and Fe-dolomite/ankerite, are primary contributors to reduction of primary intergranular porosity, alongside clay minerals, quartz, feldspar, etc. Secondary porosity resulting from dissolution and redistribution processes also significantly influences overall porosity evolution. Clay minerals, detrital and authigenic, exhibit a complex interplay with other diagenetic processes, further reducing porosity and permeability. Authigenic clay minerals, including illite, chlorite, and kaolinite, act as pore-filling cement or coatings, hindering fluid flow. Paragenetic processes delineate the intricate relationship between mineralogical transformations and petrophysical properties, defining reservoir quality. Understanding diagenetic dynamics is essential for predicting reservoir quality, fluid migration pathways, and hydrocarbon productivity. This study fills a crucial knowledge gap regarding the diagenesis of the Upper Miocene lacustrine sandstones in the southwestern part of the Pannonian Basin System, providing insights vital for the energy sector and supporting sustainable resource development in the region.

Keywords:
sandstone reservoirs; diagenesis, porosity; North Croatian Basin; Late Miocene

1. Introduction

The Upper Miocene lacustrine sandstones of the North Croatian Basin are pivotal reservoir rocks for oil and gas exploitation, not only locally but also across the broader Pannonian Basin System (**Lučić et al., 2001; Saftić et al., 2003; Dolton, 2006; Vrbanac et al., 2010; Malvić and Velić, 2011; Velić et al., 2012; Cvetković et al., 2018; Matošević et al., 2019a, b, 2021, 2023a, 2024; Kolenković Močilac et al., 2022**).

They were deposited during the Late Miocene in the brackish Lake Pannon, which was formed due to the isolation of the Central Parathetys from marine influences (**Steininger and Rögl, 1979; Báldi, 1980; Harzhauser and Piller, 2007; Harzhauser and Mandic, 2008; Ter Borgh et al., 2013; Mandic et al., 2015; Kováč et al., 2018; Magyar, 2021**). The sandstones were primarily deposited through deltaic system progradation associated with turbidites in deeper basin regions (e.g., **Magyar**

Corresponding author: Mario Matošević
e-mail address: mario.matosevic@ina.hr

et al., 1999, 2013; Ivković et al., 2000; Saftić et al., 2003; Kovačić et al., 2004; Kovačić and Grizelj, 2006; Vrbanac et al., 2010; Malvić and Velić, 2011; Sztanó et al., 2015; Balázs et al., 2018; Sebe et al., 2020; Anđelković and Radivojević, 2021). The detritus originated from the Eastern Alps orogenic belt, with sedimentary, metamorphic, and igneous rocks of the ALCAPA tectonic mega-unit, following W/NW to E/SE trajectories (**Šćavničar, 1979; Kovačić and Grizelj, 2006; Matošević et al., 2023a, 2024**).

In addition to provenance, diagenesis profoundly affects reservoir development and quality, by altering sediment post-deposition, significantly impacting petrophysical parameters (**Guohua, 1982; Civitelli et al., 2023**). It involves physical, chemical, and biological processes altering sedimentary assemblages, ranging from subaerial weathering to low-temperature metamorphism (**Curtis, 1977; Burley et al., 1985; Worden and Burley, 2003**). Understanding burial diagenesis is crucial in predicting porosity distribution, fluid migration pathways, and reservoir productivity (**Hurst, 1987**). With the increasing demand for petroleum resources, advanced recovery techniques necessitate a comprehensive grasp of diagenetic processes (**Pittman and King, 1986; Kantorowicz et al., 1992**). For instance, understanding mineral cementation, such as quartz, carbonate minerals, and clay minerals, is essential for predicting reservoir quality within a basin (**Curtis, 1983; Burley et al., 1985**). Integrating diagenetic processes throughout the sediment column is paramount for accurate reservoir characterization.

Despite longstanding importance of the Upper Miocene sandstones from the North Croatian Basin, a comprehensive understanding of their diagenesis has been lacking (e.g., **Tadej et al., 1996; Matošević et al., 2019a, 2021**). Diagenetic processes, influenced by factors such as burial depth, temperature, pressure, mineralogy, and pore fluid geochemistry, significantly shape such reservoirs (**Morad et al., 2000; Worden and Burley, 2003**). Filling this information void is crucial for the energy sector, facilitating further hydrocarbon exploration and production activities, as well as initiatives related to energy transition and environmental conservation, including carbon capture, utilization, and storage, along with expanding investments in regional geothermal energy (c.f., **Sneider, 1990; Kolenković et al., 2013; Horváth et al., 2015; Podbojec and Cvetković, 2016; Macenić et al., 2020; Alcalde et al., 2019; Tuschl et al., 2022; Vulin et al., 2023**).

In continuation of the preceding research by **Matošević et al.** (**2023a, 2024**), which provided insights into the provenance of the sandstones, this study aims to further elucidate the diagenetic processes affecting these reservoirs. This paper presents a comprehensive study on the diagenesis of the Upper Miocene sandstones in the North Croatian Basin, focusing on samples from exploration wells in the Sava and Drava depressions. Employing various methods, including petrography, scanning electron microscopy with energy-dispersive X-ray spectroscopy (SEM-EDS), X-ray diffraction (XRD), and petrophysical measurements, our objective was to identify diagenetic processes with increasing depth, including mineralogical alterations and compaction, influencing primary and secondary porosity. Additionally, we aimed to discern paragenetic sequences of diagenetic processes crucial for understanding reservoir property evolution. These insights enhance exploration and reservoir modelling efforts within the Pannonian Basin System, supporting sustainable energy resource development of the region.

2. Geological setting

The North Croatian Basin, situated in northern Croatia, is part of the Pannonian Basin System, spanning approximately 32,000 km^2 (**Figure 1**). Notably, it comprises the Sava and Drava depressions, tectonically induced and crucial depocenters during the Neogene (**Pavelić and Kovačić, 2018**; **Figure 1**).

This SW part of the Pannonian Basin System witnessed the deposition of Lower to Upper Miocene strata over tectonized Paleozoic to Paleogene basement rocks (**Pamić, 1999; Pavelić, 2001; Saftić et al., 2003; Matošević et al., 2015; Pavelić and Kovačić, 2018; Matošević and Šuica, 2017; Šuica et al., 2022a, b; Rukavina et al., 2023**), marked by significant geological changes driven by tectonic shifts, climatic fluctuations, and volcanic events (**Pavelić and Kovačić, 2018; Grizelj et al., 2020, 2023; Premec Fućek et al., 2022; Matošević et al., 2019c, 2023b**). The evolution of the Pannonian Basin System is distinguished into syn-rift and post-rift phases (**Royden, 1988; Tari et al., 1992; Matenco and Radivojević, 2012**).

The post-rift phase, characterized by diminished tectonic activity, led to lithospheric cooling, subsidence, and the isolation of the Central Parathetys from global oceans, forming Lake Pannon (**Rögl and Steininger, 1983; Royden, 1988; Tari et al., 1992; Rögl, 1998; Harzhauser et al., 2007; Piller et al., 2007; Ter Borgh et al., 2013; Kováč et al., 2017**). Intense basin subsidence and humid conditions with significant lake depths (**Sztanó et al., 2013; Balázs et al., 2018**) fostered large accumulation of post-rift siliciclastic deposits, including sandstone bodies, particularly in the central part of the depressions (**Ivković et al., 2000; Saftić et al., 2003; Kovačić and Grizelj, 2006; Malvić and Velić, 2011; Matošević et al. 2023a, 2024**).

The Upper Miocene deposits, referred to as the Pannonian in the regional Central Paratethys time scale (**Hilgen et al., 2012**), underlie Pliocene and Pleistocene (Cernikian) lacustrine and alluvial sediments and overlie Middle Miocene (Sarmatian) marine deposits (**Pavelić, 2001; Mandic et al., 2015; Pavelić and Kovačić, 2018; Kurečić et al., 2021**). They predominantly formed as

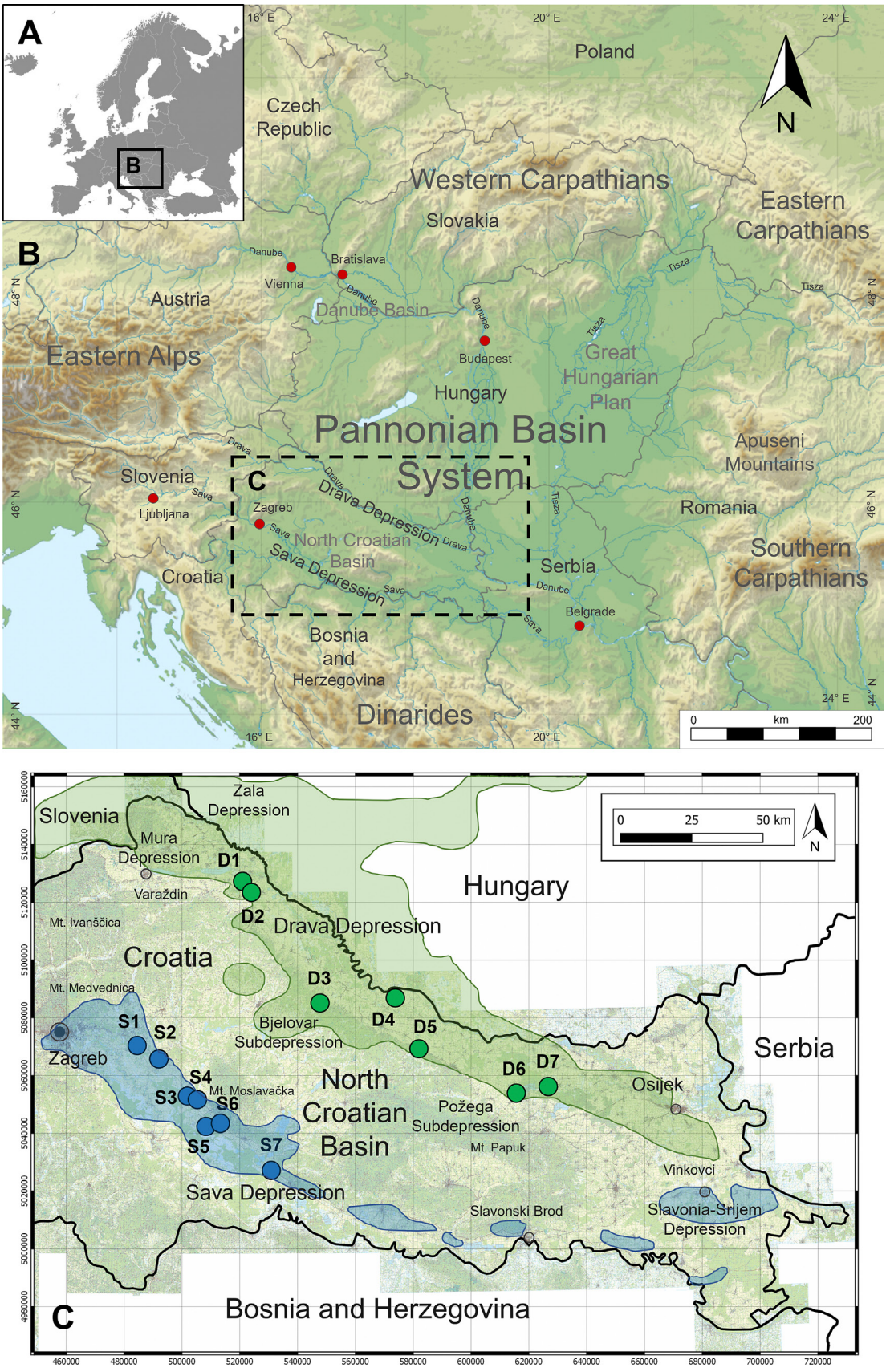

Figure 1: A – Europe with the position of the Pannonian Basin System. **B** – Geographical overview of the Pannonian Basin System in Central Europe, surrounded by the mountain ranges of the Alps, the Carpathians, and the Dinarides, with the North Croatian Basin in its SW part. **C** – Locations of the Upper Miocene reservoir sandstones from exploration wells in the North Croatian Basin within the Sava (S1-S7) and Drava depression (D1-D7).

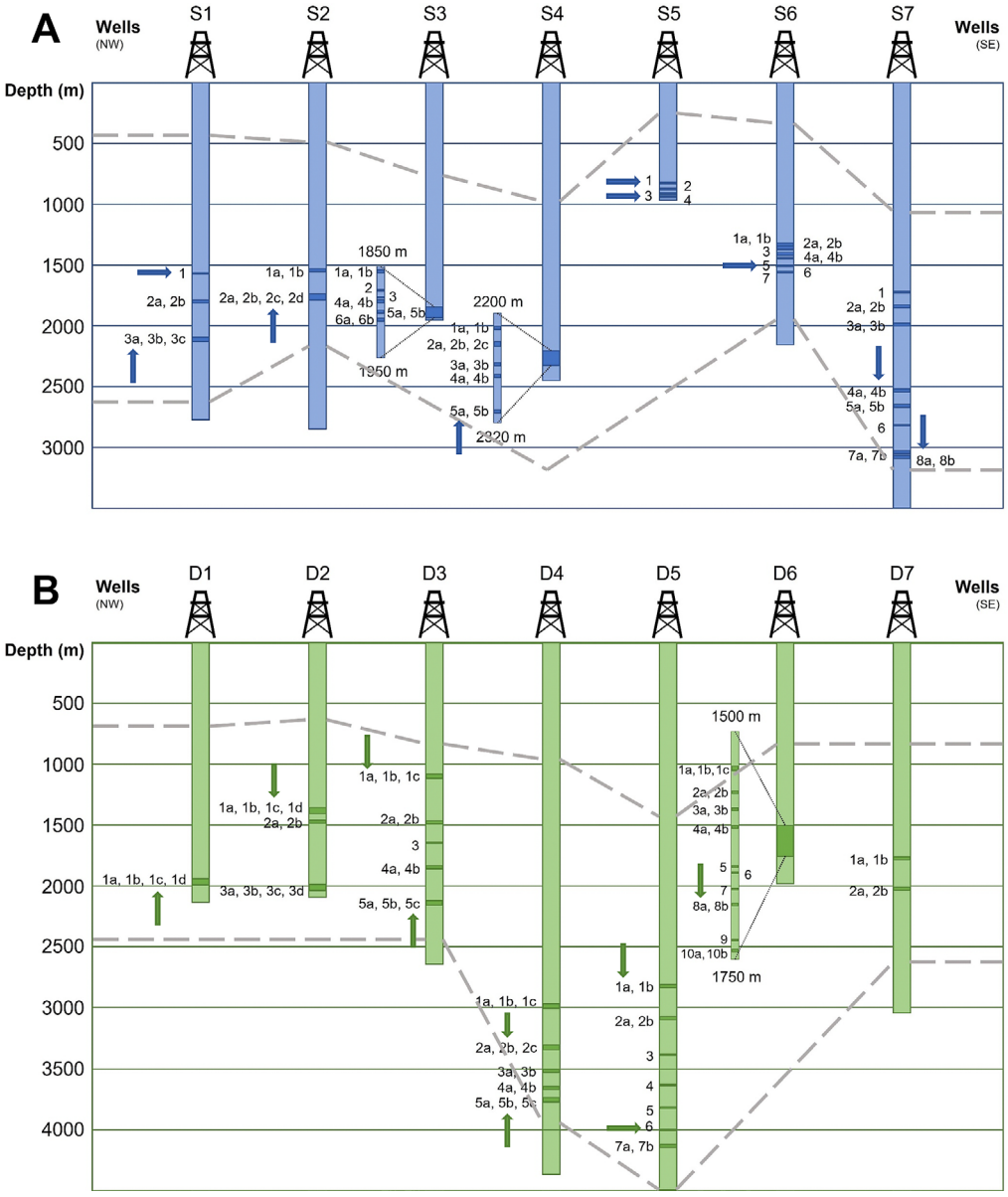

Figure 2: Positions of the Upper Miocene sandstone cores from the exploration wells in the Sava (**A**) and Drava (**B**) depressions which are the focus of the research. The stratigraphic correlation of the wells is based on the well-log data boundaries between the Upper Miocene and Pleistocene/Pliocene in shallower intervals (upper dashed line) and the Middle/Lower Miocene or the Neogene basement in deeper intervals (lower dashed line). For the geographic location of wells, see **Figure 1**. The arrows indicate the positions of core samples that were selected for detailed petrographic, SEM-EDS and XRD analyses.

turbidite mass flow deposits and later covered by delta and fluvial system deposits (**Ivković et al., 2000; Saftić et al., 2003; Magyar et al., 2013; Sztanó et al., 2015; Špelić et al., 2019, 2023; Sebe et al., 2020**).

These Upper Miocene sandstones, known for their high porosity and permeability, are key reservoir rocks in Croatia (**Lučić et al., 2001; Saftić et al., 2003; Vrbanac et al., 2010; Velić et al., 2012; Matošević et al., 2019a, b; Kolenković Močilac et al., 2022**). These sandstones were deposited in various environments including deeper-water fan lobes, channels, and levees; as well as prodelta, delta front, delta plain, and alluvial plain settings, including distributary channels and mouth bars (**Pogácsás, 1984; Juhász, 1994; Basch et al., 1995; Magyar et al., 2013; Kovačić et al., 2004; Kovačić and Grizelj, 2006; Sztanó et al., 2015; Sebe et al., 2020; Anđelković and Radivojević, 2021; Špelić et al., 2023**). Originating from a recycled orogen provenance area, these sandstones contain a diverse array of rock fragments, suggesting a complex provenance from the Eastern Alps, including the predominant Austroalpine nappe (**Šćavničar, 1979; Kovačić and Grizelj, 2006; Matošević et al., 2024**). Similar detrital signatures in both depressions suggest a shared origin within the

lake's depositional setting, possibly associated with Paleo-Sava and/or Paleo-Drava, following NW to SE transport direction of detritus (**Matošević et al., 2024**).

3. Methods

The dataset comprises 14 exploration wells from the Sava and Drava depressions, drilled by INA – Industrija nafte d.d., and a total of 130 sandstones samples from cored intervals (**Figure 2**), out of which 18 samples were analyzed for petrography, SEM-EDS, and XRD. These samples were chosen based on their representation of the Late Miocene succession of the basin infill and their suitability for comprehensive analysis of diagenetic alterations across different depth intervals. All 130 samples were utilized for petrophysical measurements, focusing on porosity. (**Figure 2**).

3.1. Petrography and SEM-EDS

The petrographic examinations involved detailed analyses of the 18 selected sandstone samples impregnated with blue-dyed epoxy and stained with Alizarin Red S. The samples were analyzed by an Olympus BX51 polarizing microscope to discern grain contacts, porosity types, and diagenetic alteration processes in thin sections.

SEM-EDS analyses provided detailed insight into microstructural features and mineralogical compositions of the 18 selected sandstone samples. The samples underwent coating with a thin layer of Au for enhanced conductivity. SEM imaging was performed using a JEOL JSM-6510 LV SEM at acceleration voltages ranging from 5 to 25 kV, revealing surface topography at magnifications ranging from 25 to 20,000x. Analysis of individual minerals, considering morphological features and chemical composition, was conducted using secondary electron (SE) and back-scattered electron (BSE) images, alongside energy-dispersive X-ray spectra (EDS) from an Oxford INCA X-act system (Oxford Instruments, High Wycombe, UK). Mineral identification relied on comparing X-ray spectra with literature data (**Welton, 1984; Severin, 2004**). SEM-EDS analyses were preformed in the Exploration & Production Laboratory in the INA – Industrija nafte d.d.

3.2. XRD

XRD was employed for the determination of clay mineral assemblage in the 18 studied sandstone samples. The samples were crushed in jaw crusher followed by pulverization in agate mortar until passing sieve opening of 0.02 mm. Prior to separation of clay fraction, the samples were treated by acetic acid to dissolve carbonates, then by hydrogen peroxide to remove organic matter and finally by Tamm solution (mixture of oxalic acid and ammonium oxalate) to eliminate Fe-Mn-Al oxides/hydroxides. The clay fraction was separated by gravitation in a centrifuge, and then deposited from suspension on glass mounts in order to obtain oriented samples for the phase analysis. Four sets of the samples were prepared: air-dried, glycolated, and heated for half an hour at 400°C and 550°C. XRD data were collected using Philips X'Pert PRO diffractometer PW 3040/60 at the Department of Geology, Faculty of Science, University of Zagreb, with CuKa radiation generated at 40 kV and 40 mA. Recording parameters were as follows: divergence slit 1/8°, antiscatter slit 1/4°, sample mask of 10 mm, Soller slits inserted into primary and diffracted beam path, scanning step 0.026°2q, and measuring time 128.27 s/step. Pixcel detector was employed for acquisition of data, which were later processed using X'Pert Highscore (**Panalytical, 2004**). Clay minerals were identified applying the following criteria: **illite** was distinguished by 10 Å peak that does not shift after glycolation and heating treatments; **chlorite** was confirmed by 14 Å and 7 Å peaks that do not shift and do not change intensity significantly after glycolation and heating treatments; **kaolinite** was identified by 7 Å peak that disappears after heating at 550°C; mutual discrimination of chlorite and kaolinite was done by spotting chlorite 004 (around 3.54 Å) and kaolinite 002 (around 3.57 Å) diffraction maxima in glycolated samples; mixed layered **illite/smectite** phases were recognized by a maximum between 10 and 14 Å and its shift toward higher d-values in glycolated samples, as well as by asymmetry of 10 Å peak; illite content in mixed-layered illite/smectite was estimated by observing the position of illite/smectite 001/002 and 002/003 diffraction maxima in glycolated samples; **illite/chlorite** was determined by 10-14 Å peak that does not change during glycolation and heating treatments; **kaolinite/smectite** was identified by 7.2-7.5 Å peak that slightly shifts and broadens to a higher d-value during glycolation while it further increases and broadens at 400°C but disappears at 550°C; **dioctahedral vermiculite** was identified by a slight increase of 14 Å peak during glycolation and its collapse to lower d-values after heating treatments (to around 12 and 11 Å); **dioctahedral illite/vermiculite** was determined by 10-14 Å peak that does not change or slightly increases during glycolation but discretely and stepwisely decreases during heating treatments (**Moore and Reylonds, 1997**). Illite crystallinity was determined by measuring the width at half maximum of 10 Å peak of glycolated samples. The method employs standardless approach that allows estimation of the illite crystallinity as described in the provenance and weathering studies (e.g., **Liu et al., 2007; Griffiths et al., 2019, and references therein**), thus enabling mutual comparison of the investigated samples in this respect. The experimental conditions for XRD recording in this case were the same as previously mentioned, and the XRD pattern profile around 10 Å peak was fitted using Panalytical X'Pert HighScore software with additional visual inspection for possible interferences of neighbouring diffraction maxima.

3.3. Porosity Measurements

Porosity measurements of sandstone samples were conducted following precise methodologies to ensure accuracy and reliability. Cylinder plugs were extracted from 130 sandstone core samples, each measuring 3.81 cm in diameter and 6 cm in length, ensuring sample uniformity. Before measurements, chloroform and methanol were used in the sample cleaning process to remove petroleum, salt, and other impurities. This step aimed to eliminate potential interference with the results. Subsequently, the samples were dried at 105°C in a conventional laboratory until they reached a constant weight, ensuring residual moisture removal without sample damage. The drying process was monitored until samples reached a constant weight.

Porosity measurements were conducted using a helium gas expansion porosimeter, relying on Boyle's law to govern gas expansion from a reference cell with a known volume to a sample cell at a constant temperature. The effective pore volume and total sample volume were determined, allowing calculation of porosity as the ratio of the pore volume to the total sample volume, expressed as a percentage (**American Petroleum Institute, 1998**).

These procedures ensured accurate determination of porosity in the sandstone samples, facilitating comprehensive analyses and interpretation of reservoir properties. However, it is essential to acknowledge potential limitations or sources of errors in the porosity measurement process, such as sample heterogeneity or gas adsorption effects, which could affect the precision of the results.

4. Results

4.1. Grain size distribution and modal composition

The Upper Miocene sandstones from the Sava and Drava depressions exhibit angular to sub-rounded grains, occasionally tabular, with average sizes of 110 μm and 150 μm, respectively (**Figure 3; Supplementary Table 1 and Supplementary Table 2**), which was already described in previous investigations (**Matošević et al., 2023a, 2024**), corresponding to very fine to fine-grained sand (**Wentworth, 1922**). Grain contacts vary from point to long and concavo-convex contacts, transitioning even to sutured contacts in more compacted sandstones at greater depths. However, point contacts are primarily contacts in all samples throughout investigated depth intervals (**Figure 3**). Grain deformations, such as bending of mica and rock fragments (particularly sedimentary and metamorphic fragments), are regularly observed in samples (**Figure 3 and Figure 4 A, B, C**). Dissolution of feldspar grains and carbonate rock fragments is evident in a good number of samples, noticeable already in shallower intervals (above 1000 m) and continuing in deeper intervals. This dissolution is closely associated with the reduced presence of carbonate (early calcite) cementation in the intergranular volume (**Figure 4 D, E, F, G, H**). The dissolution of heavy minerals has also been detected (e.g., the dissolution of staurolite and minerals belonging to the epidote group in shallower intervals and the dissolution of garnets in deeper intervals; **Figure 4 I**). Rarely, some fractured quartz grains can be found in deeper intervals. The sandstones are predominantly well- to moderately well-sorted (**Figure 3, Supplementary Table 1**). Framework petrography analyses by **Matošević et al. (2023a, 2024)** reveal quartz content ranging from 43.2% to 55.6% in the Sava depression and 46.2% to 57.7% in the Drava depression (**Supplementary Table 1 and Supplementary Table 2**). Feldspar content ranges from 11.9% to 19.1% in the Sava depression and 8.0% to 15.6% in the Drava depression, while rock fragments constitute 30.1% to 42.3% and 29.1% to 41.0% in the respective depressions (**Supplementary Table 1 and Supplementary Table 2**). Sedimentary rock fragments, notably carbonate types, dominate the rock fragment composition (**Supplementary Table 1; Figure 3 and Figure 4**), classifying the sandstones as carbonaticlastic feldspatho-litho-quartzose. Mica, chlorite, and accessory heavy minerals contribute to the overall composition. Results are provided in full detail in the **Supplementary Table 1**.

4.2. Intergranular volume

Sandstone intergranular volumes in both depressions are either unfilled or partly/entirely filled with fine-grained matrix and/or cement (**Figures 3-6**). Descriptive information about the filling of the intergranular volume for each sample can be found in the **Supplementary Table 2**.

4.2.1. Matrix

The matrix consists of silty and clayey particles derived from the breakdown and alteration of main mineral grains during transport and deposition. Phyllosilicates (mica, chlorite, and detrital clay minerals) predominate, with carbonate minerals, quartz, and feldspar also present. The matrix is in general more prominent in samples from shallower intervals in both depressions. Pseudomatrix, resulting from compaction and deformation of unstable grains during diagenesis, is occasionally observed, particularly from rock fragments like mudrocks (e.g., rip-up clasts of marl) and metasediments (**Figure 4 C**).

4.2.2. Cement

Authigenic cement mainly comprises carbonate minerals and/or a combination of carbonate minerals with clay minerals, quartz, and feldspar (**Supplementary Table 2; Figure 5 and Figure 6**).

Carbonate: Predominantly composed of calcite and Fe-dolomite/ankerite, rarely dolomite and Fe-calcite, and extremely rarely siderite (**Supplementary Table 2; Figure 3 C, D and Figure 5 A, B, C**). It often forms

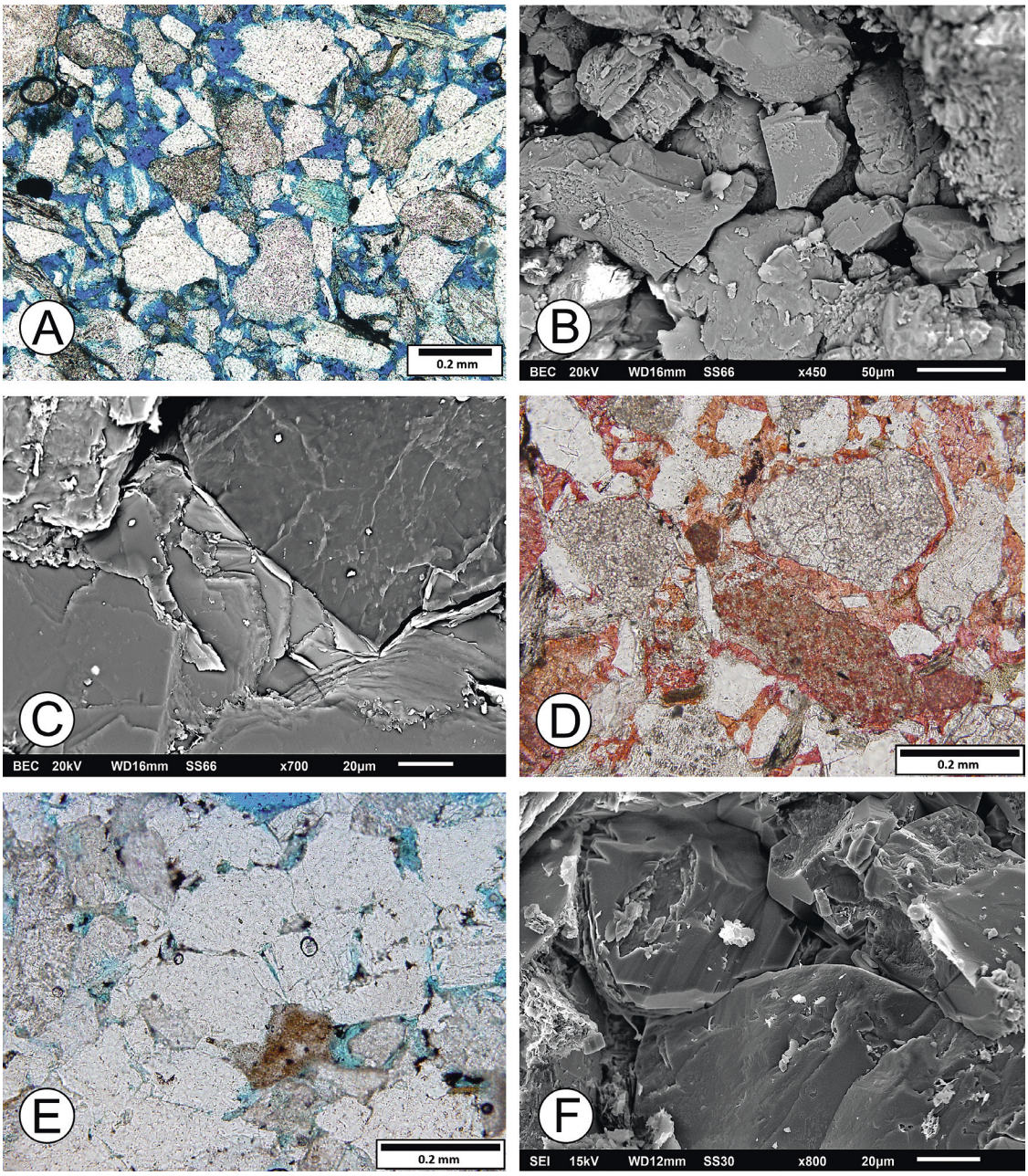

Figure 3: The Upper Miocene sandstones of the Sava and Drava depressions at low magnifications in thin sections and SEM. **A** – Sandstone impregnated with blue-dyed epoxy showing very fine to fine, angular to sub-rounded detrital grains, predominantly in point contacts, and primary intergranular porosity (S5_1, PPL); **B** – Sandstone with main grains and mostly unfilled intergranular volume with connected pores (S5_3, SEM BE); **C** – Detail of more compacted sandstone, showing densely packed grains with long contacts, grain deformations, and carbonate cement, filling the intergranular volume (S7_4b, SEM BE); **D** – The main grains in the sandstone consist of quartz, feldspars and rock fragments (mostly sedimentary rock fragments in the form of recrystallized carbonates), and the cement is calcite, stained with Alizarin Red S (S1_1, PPL); **E** – Rearrangement of grains in the sandstone due to overlying pressure (compaction and deformation), reducing primary intergranular porosity with precipitation of cement on grain surfaces and within pores, but also dissolving some grains with formation of secondary porosity (D3_5c, PPL); **F** – Grains in mutual penetrant (concavo-convex) contacts, partly due to later cement overgrowing on primary detrital grains (D1_1c, SEM SE). PPL = plane-polarized light, SEI = secondary electron image, BEI = backscattered electron image. Photo: M. Matošević.

rhombohedral crystals in intergranular space (**Figure 5 B**), sometimes in conjunction with other authigenic minerals. Authigenic carbonates create euhedral overgrowths on detrital carbonate grains and partly/completely fill pores as well (in some samples early calcite sparry cement extends from grain to grain; **Figure 3 C, D and Figure 5 A**). It does not clearly depend on depth, although tightly cemented sandstones were mainly found in deeper intervals of the depressions, especially in the Drava depression. Fe-dolomite/ankerite generally

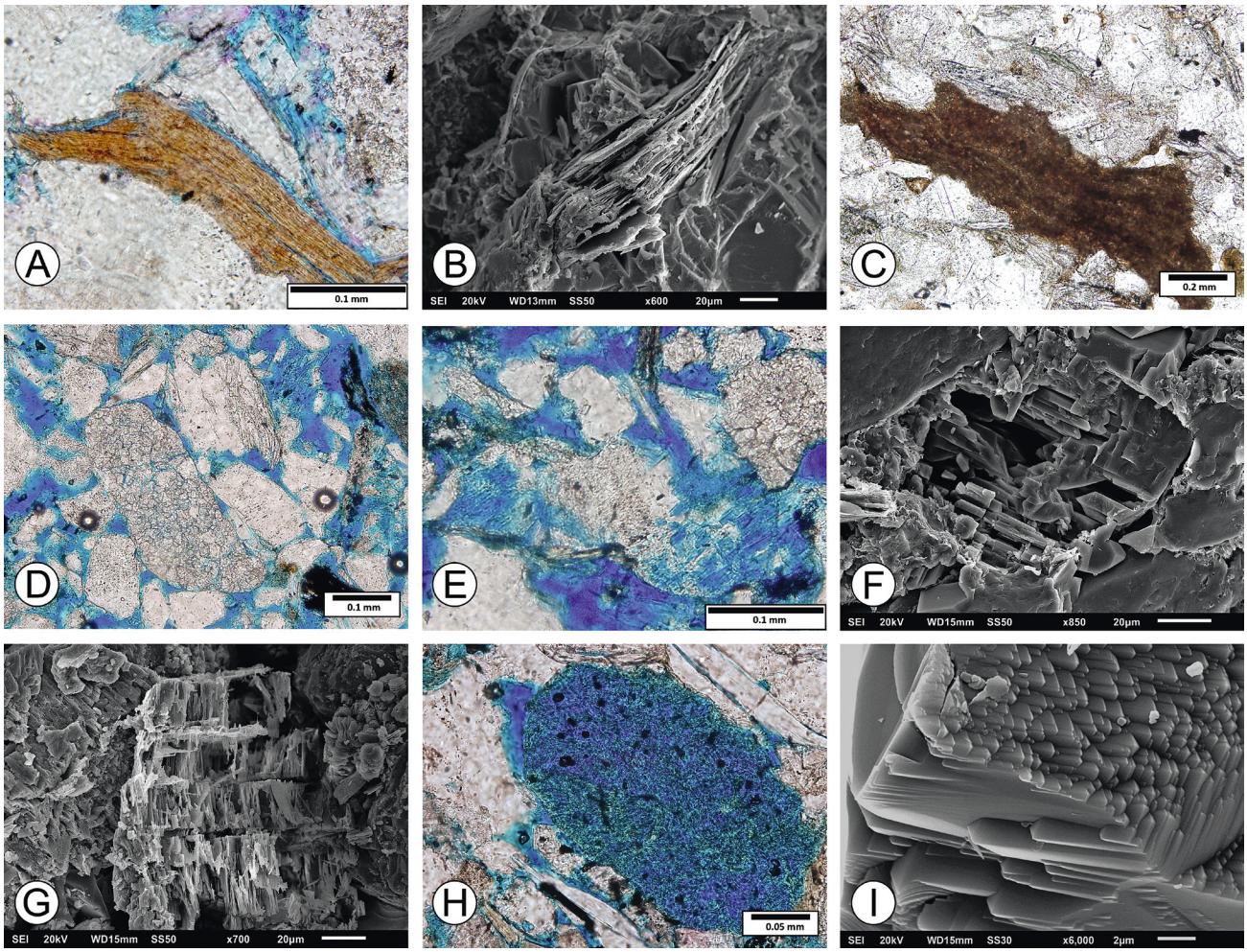

Figure 4: Diagenetic alterations of grains in the Upper Miocene sandstones of the Sava and Drava depressions in thin sections and SEM. **A** – Deformation (bending) of biotite due to compaction, locally making obstacles for fluid flow (D3_5c, PPL); **B** – Simultaneous deformation and decomposition of muscovite and formation of secondary dissolution porosity (S1_1, SEM SE); **C** – Formation of pseudomatrix by compaction and deformation of unstable grains (mudrock rock fragment) (S6_5, PPL); **D** – Intragranular porosity stemming from partial dissolution of recrystallized carbonate rock fragment (D2_1c, PPL); **E** – Secondary pores impregnated with blue-dyed epoxy in party dissolved alkali feldspar contributing to overall porosity (D2_1c, PPL); **F** – Pore formation due to dissolution of Na-plagioclase (S4_5a, SEM SE); **G** – Resorption of Na-Ca plagioclase with preferred orientation of the remnants signifying that dissolution of the grain was crystallographically controlled (S6_5, SEM SE); **H** – Complete dissolution of detrital grain (possibly volcanic rock fragment) with clay mineral replacement, promoting secondary porosity and microporosity (S4_5a, PPL); **I** – Skeletal garnet with deeply etched faceted grain surface as a result of dissolution (D3_1a, SEM SE). PPL = plane-polarized light, SEI = secondary electron image. Photo: M. Matošević.

occurs in samples from intervals deeper than 1000 m in both depressions.

Quartz: Largely manifested as authigenic quartz overgrowths on detrital quartz grains. It primarily forms well-developed crystals with smooth euhedral faces, partly/completely surrounding quartz grains (**Supplementary Table 2; Figure 5 D, E, F**). Occasionally, it also occurs as pore-linings and pore-fillings with other minerals (primarily clay minerals), predominantly in the form of microcrystalline quartz, with a multitude of small bipyramidal crystals generally less than 10 µm length (**Figure 5 G**). In general, quartz cement arises in samples from intervals deeper than 1000 m in both depressions.

Feldspar: Relatively sporadic, appearing as authigenic overgrowths of alkali feldspar and plagioclase (mainly Na-plagioclase) in the form of small poorly to well-developed crystals (**Figure 5 H**), sporadically also corroded. Na-plagioclase cement is observed from shallower intervals in both depressions, but with notable amount mostly in samples deeper than 2000 m.

Pyrite: Exceptionally rare, manifested usually as microcrystalline subhedral to euhedral framboids in clusters, together with other authigenic minerals (**Figure 5 I**). It appears mainly in samples from deeper intervals in both depressions, usually far deeper than 2000 m.

Clay Minerals (detrital and authigenic): Mainly illite, chlorite, kaolinite, and mixed-layered clays, observed as

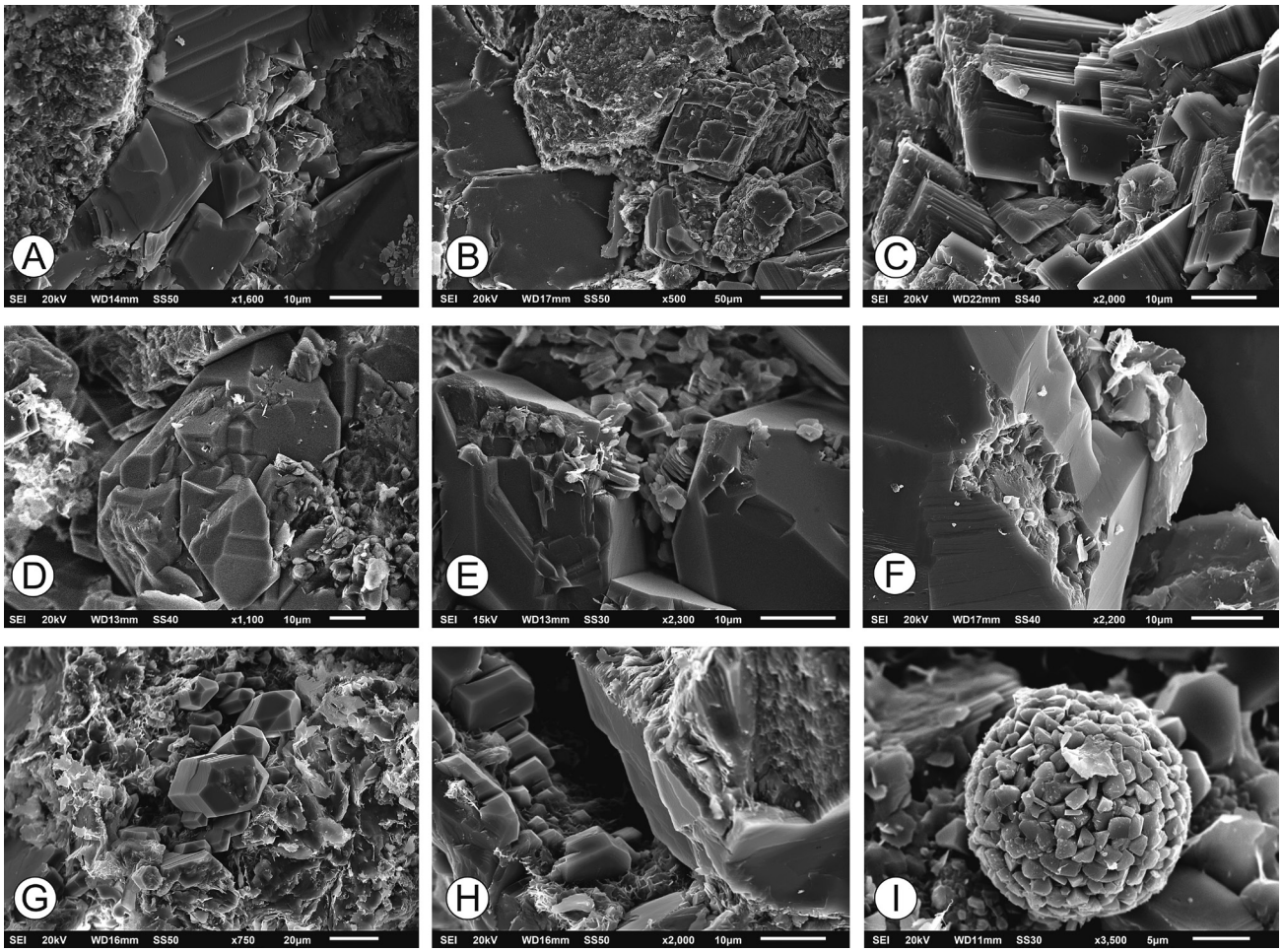

Figure 5: Cements in the Upper Miocene sandstones of the Sava and Drava depressions in SEM. **A** – Authigenic calcite in combination with clay minerals expanding from grain to grain (D4_2b, SEM SE); **B** – Rhombohedral crystals of Fe-dolomite/ankerite in pore space contributing to the reduction of porosity and local permeability (S4_5a, SEM SE); **C** – Calcite crystal overgrowths on detrital carbonate grain enlarging to intergranular space (S7_8a, SEM SE); **D** – Quartz cement manifesting as authigenic quartz overgrowth completely surrounding detrital quartz grain (D1_1c, SEM SE); **E** – Euhedral smooth quartz overgrowth on detrital quartz grain with clay minerals in intergranular volume (D1_1c, SEM SE); **F** – Quartz grain enclosed in incomplete well-developed quartz overgrowth (S4_5a, SEM SE); **G** – Microcrystalline quartz crystals with clay minerals lining intergranular pores (D3_5c, SEM SE); **H** – Pore-lining microcrystalline Na-plagioclase overgrowths with clay minerals (D3_5c, SEM SE); **I** – Framboidal pyrite (D1_1c, SEM SE). SEI = secondary electron image. Photo: M. Matošević.

coatings, pore fillings, or matrix components (**Supplementary Table 2 and Supplementary Table 3; Figure 6 and Figure 7**). Illite is principally observed as flakes and fibrous structures on the surface of detrital grains, at the edges of phyllosilicates and rock fragments, dispersed through the matrix, or as pore-filling clusters (**Figure 6 A, B**). Detrital illite typically exhibits irregular, flake-like platelets oriented parallel to each other, while authigenic illite appears mostly in the form of filaments and/or ribbons, often lining and bridging pores (**Figure 6 A, B**). Authigenic illite appears mainly from 2000 m deeper in both depressions. Chlorite is found as detrital particles, usually as individual flakes with parallel face-to-face orientations, formed through alterations of mica and chlorite in shallower intervals, or as authigenic minerals, frequently as clusters of elongate to disc-like crystals partly filling pores and rarely as pore-lining, forming thin rims around detrital grains with euhedral crystals differently oriented and perpendicular to the grain surface (**Figure 6 C, D**). Authigenic chlorite significantly occurs in samples from 2500 m deeper in the Sava depression and samples from 2000 m deeper in the Drava depression. Kaolinite predominantly appears in clusters within pores or adhering to detrital grains, originating from the decomposition of the grains (generally feldspars), occasionally exhibiting a vermiform structure (**Figure 6 E, F**). Kaolinite was predominantly recognized as authigenic, well-crystallized face-to-face stacks of hexagonal and pseudo-hexagonal plates or booklets (**Figure 6 G**). It occurs in samples from shallower intervals, above 1000 m, but continues in samples from deeper intervals as well in both depressions. Correspondingly to occurrence of feldspar dissolution, it is mainly found in samples which have no pronounced early calcite cementation. In samples from deeper intervals, dickite (blocky kaolinite) is also observed. Among mixed-layered and other clays, most

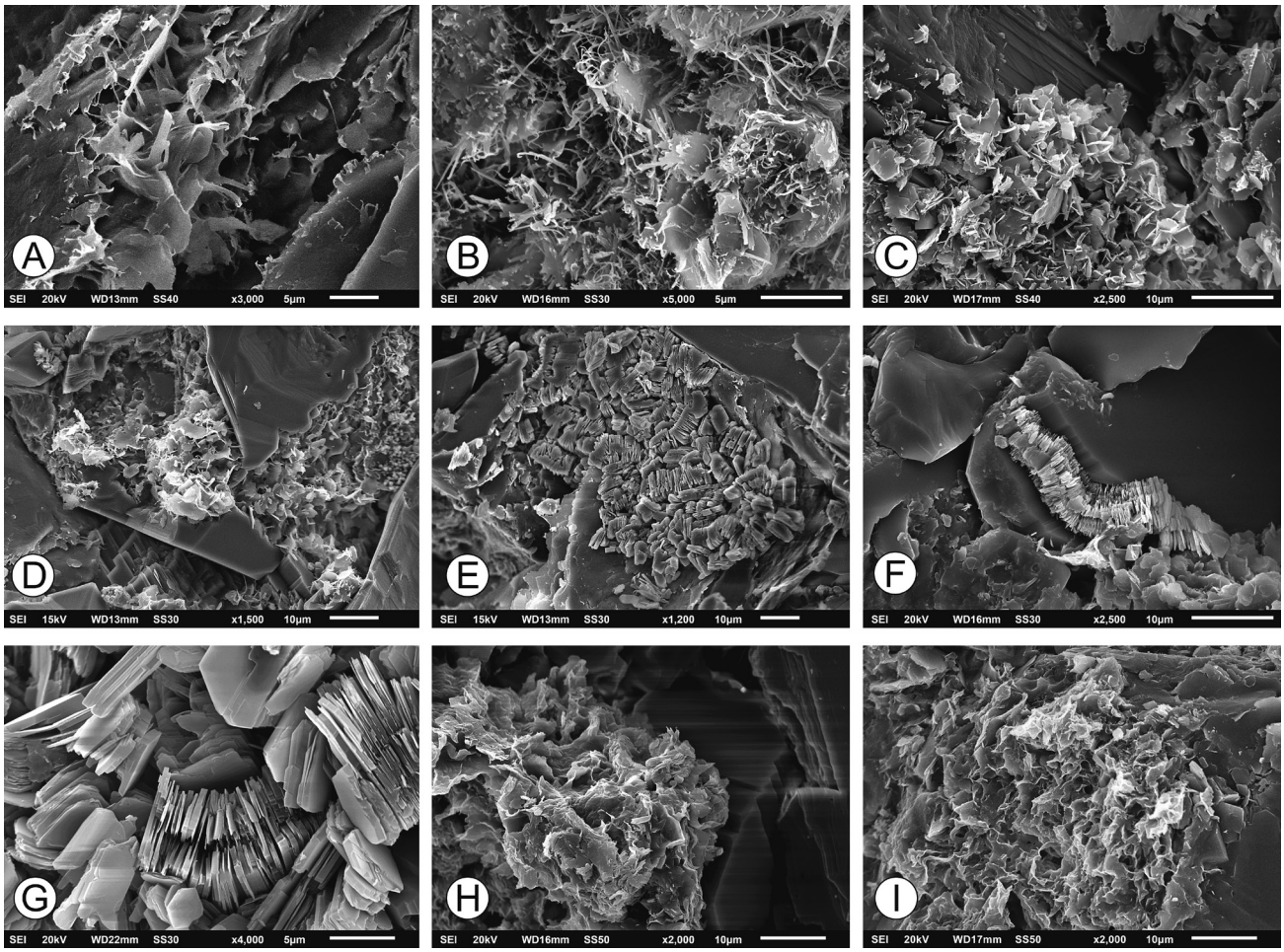

Figure 6: Clay cements in the Upper Miocene sandstones of the Sava and Drava depressions in SEM. **A** – Illite as flakes and fibrous structures on the surface and at the edges of muscovite, expanding to intergranular space (D1_1c, SEM SE); **B** – Filamentous pore-lining and pore-bridging authigenic illite (D3_5c, SEM SE); **C** – Cluster of authigenic chlorite to illite/chlorite partly filling pore (S7_4b, SEM SE); **D** – Chlorite forming rims around detrital quartz grain preventing quartz overgrowth (D1_1c, SEM SE); **E** – Cluster of kaolinite minerals within pore (D1_1c, SEM SE); **F** – Vermiform kaolinite adhering to detrital grain (S2_2c, SEM SE); **G** – Detailed view of authigenic kaolinite with face-to-face stacks of pseudo-hexagonal plates (S1_3a, SEM SE); **H** – Cluster of illite/smectite to illite in intergranular space (S2_2c, SEM SE); **I** – Rim of illite/smectite on detrital grain (D2_1c, SEM SE). SEI = secondary electron image. Photo: M. Matošević.

prevalent illite/smectite (**Figure 6 H, I**), illite/chlorite, chlorite/smectite, kaolinite/smectite, dioctahedral vermiculite, and dioctahedral illite/vermiculite are identified based on XRD analyses (**Figure 7**). Questionable occurrences have illite/vermiculite and sepiolite, each in only one sample. For detail clay mineral determination, refer to the results of the XRD analyses (**Supplementary Table 3; Figure 7**).

4.3. Porosity

Porosity measurements conducted in the Sava and Drava depressions reveal distinctive statistical parameters reflecting reservoir characteristics at specific depths. Within the Sava depression, porosity in analyzed samples ranges from a minimum of 3.0% at 3047.55 m depth to a maximum of 34.9% at 827.7 m depth, with a mean value of 19.06% and a median of 19.00%. Correspondingly, within the Drava depression, porosity in analyzed samples ranges from a minimum of 1.9% at 4141.15 m depth to a maximum of 28.7% at 1398.6 m depth, with a mean value of 14.19% and a median of 13.80%. **Supplementary Table 4** summarizes porosity measurements in both depressions, highlighting the variability across depths and underscoring the heterogeneity of subsurface reservoirs. Relationship of porosity and depth in the Sava and Drava depressions is illustrated in **Figure 8**.

Primary intergranular porosity predominates across all sandstone samples (**Supplementary Table 2; Figure 3 and Figure 4**). As mentioned earlier, the intergranular volume manifests as unfilled, partially filled, or completely filled with carbonate minerals, fine-grained matrix, different types of clay minerals, quartz, and feldspar. Pore diameters typically range from 5-100 μm, with an average size falling within the range of 10-40 μm in both depressions (**Supplementary Table 2; Figure 3 and Figure 4**). While most pores exhibit connectivity or partial connectivity, non-connected pores are discernible as

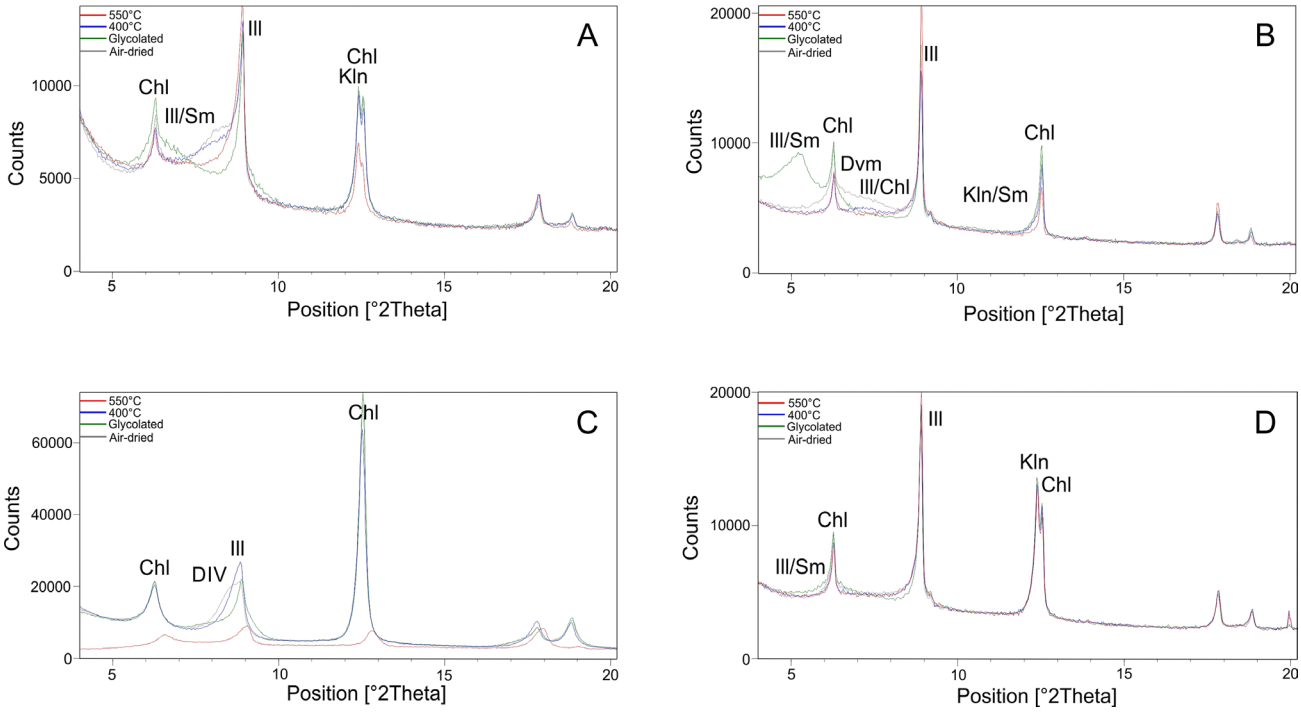

Figure 7: XRD patterns of main clay minerals in in the Upper Miocene sandstones of the Sava and Drava depressions: **A** – Sample S4_5a; **B** – Sample S5_3; **C** – Sample D4_5b; **D** – Sample D6_8a. Chl = chlorite, Dvm = dioctah. vermiculite, DIV = dioctah. Illite/vermiculite, Ill = illite, Ill/Sm = illite/smectite, Ill/Chl = illite/chlorite, Kln = kaolinite, Kln/Sm = kaolinite/smectite.

well, particularly within samples where carbonate cement establishes grain-to-grain bonds. Secondary porosity, stemming from partial to complete dissolution of detrital grains and cements is chiefly evident in feldspars (both alkali feldspars and plagioclase; **Figure 4 E, F, G**) and phyllosilicates (mica and chlorite; **Figure 4 A, B**), with sporadic occurrences within rock fragments (predominantly carbonates; **Figure 4 D**), and is infrequently also associated with cement (carbonate and feldspar cements). Micropores are present as diminutive pores (less than 2 μm), primarily linked with matrix within intergranular spaces or differently oriented detrital and authigenic clay minerals (**Figure 4 and Figure 6**), collectively contributing to overall porosity. Fracture porosity, manifested as void spaces within natural fractures, is particularly rare within samples, primarily macroscopically observed in the deepest intervals.

5. Discussion

5.1. Uniformity of sandstones and diagenetic alterations

The sandstones within the Sava and Drava depressions exhibit remarkable similarities in grain size distribution, mineralogical composition, and diagenetic alterations (**Supplementary Tables 1-3; Figures 3-7**). This uniformity in grain shape and modal composition suggests the shared provenance for the detrital material previously investigated by **Matošević et al. (2023a, 2024**). This study further elucidates comparable diagenetic processes within the depressions, particularly highlighting the compaction progressions and cementation that significantly influence sandstone porosity. As sandstone layers compact over time under the pressure of overlying sediments, intergranular spaces diminish, leading to a reduction in porosity with depth (**Figure 3 and Figure 8**). Various grains undergo rearrangement during shallow and deep burial, with ductile grains (e.g., volcanic rock fragments, mudrock intraclasts, metasediments, and phyllosilicates; **Figure 3 and Figure 4**) and matrix/pseudomatrix (**Figure 4 C**) plastically deforming, while others partially dissolve (e.g., feldspar and carbonate rock fragments; **Figure 4**) or may even fracture (e.g., quartz). These processes contribute to overall compaction of sandstones (**Waugh, 1971; Pittman and Larese, 1991; Bjørlykke and Egeberg, 1993; Worden et al. 1997; Worden and Burley, 2003**). Additionally, chemical compaction, including pressure dissolution of silicate minerals present in the sandstones, also contributes, but less significantly, to porosity reduction with increasing burial depth (**Robin, 1978**).

5.2. Grain contacts, compaction dynamics, and cementation

Examination of grain contacts reveals a spectrum of contact types evolving through compaction and associated pressure dissolution processes, ranging from point-contacts to interpenetrative (even sutured) contacts (**Fig-**

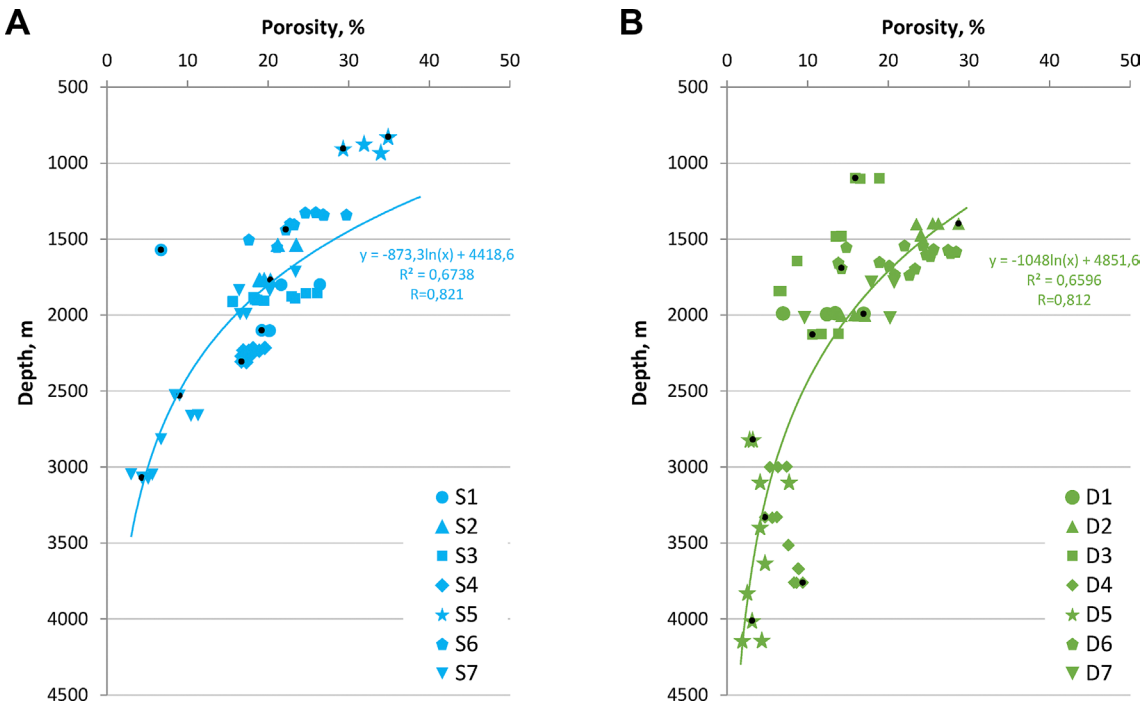

Figure 8: Depth-wise distribution of porosity values in the Upper Miocene sandstones of the Sava (**A**) and Drava (**B**) depressions, showing reductions in porosity with depth. Black dots indicate samples that underwent detailed petrographic, SEM-EDS and XRD analyses. For detailed measurement values per depth per sample, refer to the **Supplementary Table 4**.

ure 3). The dynamic nature of compaction highlights the significance of comprehending the evolution of grain contacts, which promote the development of more extensive contacts over time and depth (**Taylor, 1950; Robin, 1978**). Moreover, water expulsion during compaction facilitates cementation, with quartz and carbonate cements emerging as prominent contributors to porosity reduction in the sandstones within both depressions, manifesting in various forms (**Figure 3 and Figure 5**). Quartz overgrowths and microcrystalline quartz cement contribute to pore space reduction (**Figure 5**), particularly at burial diagenesis temperatures surpassing 70°C (**Bjørlykke and Egeberg, 1993**). Quartz cement predominantly occurs in sandstones deeper than 1000 m, with the expected temperatures in the subsurface resulting from elevated geothermal gradient within the North Croatian Basin (e.g., **Cvetković et al., 2019; Macenić et al., 2020; Tuschl et al., 2022**). Carbonate cement, primarily composed of calcite and Fe-dolomite/ankerite, significantly influences porosity reduction during both eogenesis and mesogenesis in the sandstones from both depressions (**Figure 3 C, D and Figure 5 A, B, C**). Calcite typically represents the early eogenetic grain-to-grain pore-filling cement fabrics, precipitating from pore waters post-deposition, irrespective of the primary mineralogy of the sandstones (**Figure 3 D and Figure 5 A**). Late-stage calcite cement and Fe-dolomite/ankerite are typically associated with dissolution and recrystallization of pre-existing carbonate minerals, including carbonate rock fragments, and cements, and precipitation from pore fluids in deeper intervals (**Worden and Burley, 2003, and references therein**). Fe-dolomite/ankerite, and infrequently Fe-calcite, dominate among carbonate cements during mesogenesis, crystallizing at temperatures approximately 100°C (**Morad, 1998; Worden and Burley, 2003**), and locally fill pores and pore throats in the form of rhombohedral crystals, thereby contributing to the reduction of porosity and local permeability of the sandstones (**Figure 5 B**). Some burial calcite and Fe-dolomite/ankerite cement may also originate from crystallization due to mass fluid and solute transfer, migrated from organic mudrocks intercalated with sandstones in the basin (**Jackson and Beales, 1967; Baines et al., 1991**). Additionally, it is known that oil can also influence carbonate cementation, particularly during biodegradation and oxidation processes (**Ehrenberg and Jakobsen, 2001**). Calcite and Fe-dolomite/ankerite cements emerge as the predominant factors responsible for porosity reduction in the Upper Miocene sandstones of the Sava and Drava depressions.

5.3. The role of clay minerals

The clay mineral assemblage in both the Sava and Drava depressions exhibits similar major components, including illite, chlorite, kaolinite, and other identified species (**Supplementary Table 2 and Supplementary Table 3; Figure 6 and Figure 7**), independent of sample depth. However, SEM observations indicate a shift from detrital to authigenic clays with increasing depth. Authigenic clay minerals play a crucial role in altering pore space and fluid flow within the sandstones (**Worden and Burley, 2003**). They primarily act as pore-filling cement or coatings on the main grains.

Diagenetic illite, especially fibrous types formed at temperatures above 70°C (**Figure 6 A, B**), is associated with potassium-bearing formation waters, significantly reducing permeability by blocking pore throats and reducing pore networks without notably affecting porosity (**Neasham, 1977; Warren and Curtis, 1989**). Authigenic chlorite typically formed below 2000 m depth (with temperatures exceeding 90–100°C; **Ehrenberg, 1993; Aagaard et al., 2000**). As coatings on mineral grains, chlorite decreases porosity and permeability by clogging pore throats and reducing pore network connectivity (**Figure 6 C**). Conversely, in deeper intervals, it may locally inhibit quartz cementation by preventing quartz overgrowths (**Figure 6 D**). Kaolinite is commonly clustered within pores or adhering to primary grains from shallower intervals (**Figure 6 E, F, G**), resulting from the decomposition of primary grains like feldspars. It has a dual effect on porosity and permeability – reducing primary intergranular, but locally increasing secondary intragranular porosity. Kaolinite is more abundant in samples with higher porosity, i.e., in samples having less carbonate cement, and is usually absent in the deepest horizons, especially in the Drava depression (**Supplementary Table 3**). Additionally, the reaction of kaolinite with K-feldspar to produce illite and quartz is significant, particularly at temperatures higher than about 70°C but becomes pervasive at temperatures exceeding 130°C (**Worden and Burley, 2003**). Moreover, kaolinite, typical of weathering profiles and early diagenesis, forms vermiform masses that occupy and locally fill pores, with possible replacement by chlorite in deeper potassium-deficient systems. Highly saline water and common aqueous metals, such as Na, K, Ca, and Mg, can locally affect clay, carbonate, and feldspar mineral stability in the sandstones, causing various diagenetic changes, such as additional albitization of K-feldspar and illitization of smectite and kaolinite (**de Caritat and Barker, 1992; Worden et al., 1999**). These results to some extent coincide with those obtained from the earlier study on the pelitic sediments from the Sava depression (c.f., **Grizelj et al., 2011**), particularly concerning the composition and alteration of clay minerals and carbonates with increasing depth – e.g., smectite, kaolinite, and calcite are gradually replaced by illite-smectite, illite, chlorite, Ca-dolomite/ankerite, and albite in deeper intervals of exploration wells.

Variations in mixed-layered clay species occur, with illite/smectite being the most frequent, followed by illite/chlorite. The presence of illite/smectite, though widespread, is generally absent at depth intervals around 2500-3000 meters. Although the replacement of smectite by illite in sandstones accompanies early stages of oil generation, illite content in illite/smectite remains relatively consistent depthwise in the sandstones (**Supplementary Table 3**), likely due to conflicting influences of detrital and authigenic illite. Illite crystallinity follows a more regular pattern throughout the drilled sections, with higher crystallinity observed in shallower horizons, possibly inherited from detrital illite, while crystallinity decreases in deeper horizons due to diagenetic changes. Illite/chlorite occurrence was recorded only in the Sava depression sample set, less prominent in the intervals 1500-2300 m in depth (**Supplementary Table 3**). Other clays are sparse: kaolinite/smectite and dioctahedral vermiculite were observed only in two samples from the shallowest horizons of the Sava depression, likely detrital and indicating transitional stages in clay mineral formation during weathering; dioctahedral illite/vermiculite seems more widespread among the samples of both depressions but generally occurs at deeper horizons, suggesting fine changes in mixed layered phases caused by diagenesis (**Supplementary Table 3**).

Smectite clay minerals and their interstratified types, known for reducing permeability due to their small grain size and swelling properties (**Hermanns Stengele and Plötze, 2000**), are prevalent in shallower horizons (**Supplementary Table 3**). However, aforementioned illite and chlorite abundance can also significantly reduce permeability through the drilled sections.

Furthermore, common feldspar mineral cements and overgrowths on main grains in the Upper Miocene sandstones from both the Sava and Drava depressions, although much less abundant than quartz and carbonates, also contribute to pore-filling cements (**Figure 5 H**), with burial diagenesis promoting their stability (**Morad et al., 1989**). The rarely present pyrite cement (**Figure 5 I**), usually formed under the microbial reduction of ferric iron and sulphates due to influx of saline water and reduction of hematite in the presence of hydrocarbons during both eogenesis and mesogenesis (**Love, 1967; Elmore et al., 1987**), has an insignificant impact on porosity reduction in the sandstones from both depressions.

5.4. Porosity evolution and reservoir quality

Understanding porosity in sandstones involves a complex interplay of depositional, compaction, and cementation processes (**Worden et al., 2000**). The changes in porosity observed with depth in both depressions underscore the cumulative effects of grain rearrangement, compaction, and cementation, emphasizing the dynamic nature of diagenetic processes shaping these reservoirs' properties. Initially, primary intergranular porosity dominates in both depressions (**Figure 3 and Figure 4**), with observable reduction in intergranular pore sizes with depth. Furthermore, it is observed that secondary porosity, resulting from dissolution and redistribution processes, plays a significant role in the overall porosity evolution of the studied sandstones, which conforms with the observations reported by **Schmidt and McDonald, 1979** and **Giles and de Boer, 1990**. This secondary porosity is primarily associated with feldspar, pyllosilicates, and carbonate rock fragments (**Figure 4 B, D, E, F, G**). Additionally, microporosity, primarily at-

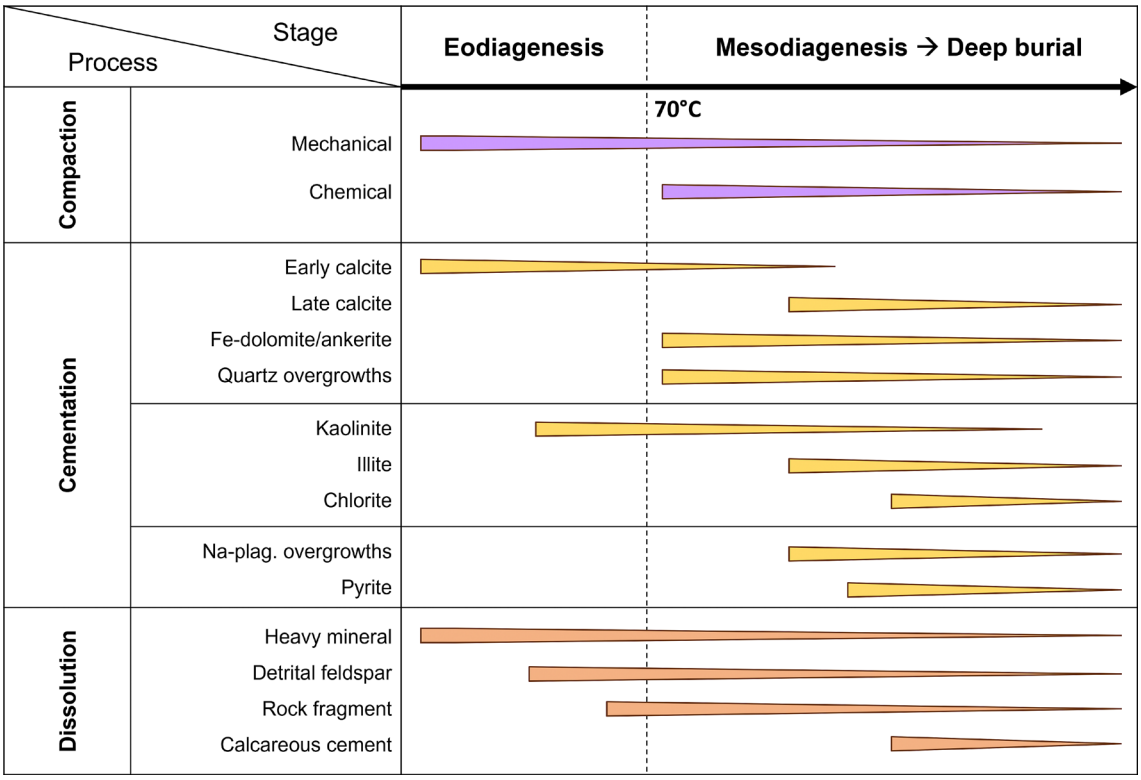

Figure 9: Generalized paragenetic sequence of diagenetic processes in the Upper Miocene sandstones of the North Croatian Basin based on analyzed samples from the Sava and Drava depressions. The same diagenetic processes (compaction, cementation, and dissolution) were observed in both Sava and Drava depressions.

tributed to matrix within intergranular spaces or variously oriented detrital and authigenic clay minerals (**Figure 6**), contributes collectively to overall porosity. Notably, the dissolution of heavy minerals which was documented at deeper sections of studied sandstones (**Matošević et al., 2023a, 2024**) does not significantly affect the overall proportion of porosity (**Figure 4 I**).

Established relationship between porosity and depth of the studied sandstones, suggests a heterogeneous nature of the Upper Miocene reservoirs' quality within the study area (**Supplementary Table 4; Figure 8**). Relatively strong relationship between porosity and depth in both depressions implies that compaction plays a significant role in porosity reduction of studied sandstones (**Figure 8**), but also that influence of other diagenetic processes generally intensifies with depth. The close alignment between mean and median values indicates a relatively even distribution of data around the central value, with no significant outliers disproportionately influencing the mean.

Moreover, the identified diagenetic paragenetic sequences unveil the intricate interplay between mineralogical transformations and evolution of petrophysical properties (**Figure 9**), ultimately defining reservoir quality and potential production (**Worden and Morad, 2000**). These findings underscore the importance of considering diagenetic processes in understanding reservoir quality and the potential implications for production strategies in the broader context of the Pannonian Basin System and similar geological settings. Further research in this field is warranted to refine our understanding of these processes and their implications for reservoir management and exploration efforts.

6. Conclusions

This study sheds light on the diagenetic evolution of the Upper Miocene lacustrine sandstones in the North Croatian Basin, providing insights into their reservoir characteristics relevant for geoenergy potential. Uniform diagenetic processes were found in both the Sava and Drava depressions, with carbonate cementation, especially calcite and Fe-dolomite/ankerite, being the main contributors to porosity reduction, along with other cements like clay minerals, quartz, feldspar, and pyrite. Compaction-induced porosity reduction, evidenced by evolving grain contacts and pressure dissolution, is widespread, leading to decreased porosity with depth. Porosity measurements confirm this trend, with values decreasing from 34.9% to 3.0% in the Sava depression and from 28.7% to 1.9% in the Drava depression, respectively. Primary intergranular porosity predominates, with secondary porosity, mainly intragranular from dissolution processes, also significant. Pore diameters typi-

cally range from 5-100 µm. Microporosity is particularly attributed to matrix, some detrital grains, and differently oriented clay minerals. The observed paragenetic sequences elucidate the intricate relationship between mineralogical transformations and evolution of petrophysical properties of the reservoirs. Clay minerals, both detrital and authigenic, interact in a complex manner with other diagenetic processes, further influencing porosity and permeability. The main clay minerals identified include illite, chlorite, kaolinite, and mixed-layered illite/smectite. Authigenic clay minerals appear at specific depths, acting as pore-filling cement or coatings on mineral grains, and additionally inhibit fluid flow. Variations in mixed-layered clay species reflect the dynamic nature of diagenetic processes. These findings highlight the complexity of diagenetic interactions and their implications for reservoir quality and potential productivity. Understanding these processes is crucial for predicting reservoir quality and fluid migration pathways. This study also highlights the need for future exploration, particularly concerning permeability measurements and the interaction of diagenetic changes and permeability of the sandstones at various depths. A more extensive sampling and exploration wells network should be included in further studies to gain a broader understanding of the Upper Miocene sandstone reservoirs' quality and their differences between depressions in the North Croatian Basin and wider Pannonian Basin System.

Acknowledgment

The authors gratefully acknowledge the support of the Faculty of Mining, Geology and Petroleum Engineering, University of Zagreb, for the Mario Matošević PhD scholarship. This research was conducted as part of the SEDBAS project, funded by the Croatian Science Foundation (IP-2019-04-7042). Special appreciation is extended to the INA – Industrija nafte d.d. for their essential contribution to this study. Additionally, we would like to thank Ljiljana Kirin and Ninoslav Sabol for their assistance with sampling and sample preparation. Our thanks are also extended to Sanja Šuica for the thorough and invaluable pre-review examination of the manuscript before the submission. Finally, we express our gratitude to Eva Mencin Gale and two anonymous reviewers for their constructive feedback, which greatly enhanced the quality of the manuscript.

7. References

Aagaard, P., Jahren, J., Harstad, A.O., Nilsen, O. and Ramm, M. (2000): Formation of grain-coating chlorite in sandstones. Laboratory synthesized vs. natural occurrences. Clay Minerals, 35, 261-269.

Alcalde, J., Heinemann, N., Mabon, L., Worden, R.H., de Coninck, H., Robertson, H., Maver, M., Ghanbari, S., Swennenhuis, F., Mann, I., Walker, T., Gomersal, S., Bond, C.E., Allen, M.J., Haszeldine, R.S., James, A., Mackay, E.J., Brownsort, P.A., Faulker, D.R. and Murphy, S. (2019): Acorn: Developing full-chain industrial carbon capture and storage in a resource- and infrastructure-rich hydrocarbon province. Journal of Cleaner Production, 233, 963-971. doi: 10.1016/j.jcanlepro.2019.06.087

American Petroleum Institute (1998): Recommended Practice for Core Analysis (RP-40), 2nd edition, API, API Publishing Service, Washington.

Anđelković, F. and Radivojević, D. (2021): The Serbian Lake Pannon formations - their significance and interregional correlation. Geološki anali Balkanskog poluostrva, 82, 2, 43-67. doi: 10.2298/GABP210420007A

Baines, S.J., Burley, S.D. and Gize, A.P. (1991): Sulphide mineralization and hydrocarbon migration in North Sea oilfields. In: Pagel, M. and Leyroy, J. (Eds.): Source, Transport and Deposition of Metals, 507-511. Balkema, Rotterdam.

Balázs, A., Magyar, I., Matenco, L., Sztanó, O., Tőkés, L. and Horváth, F. (2018): Morphology of a large Palaeo-lake: Analysis of compaction in the Miocene-Quaternary Pannonian Basin. Global and Planetary Change, 171, 134-147. doi: 10.1016/j.gloplacha.2017.10.012

Báldi, T. (1980): A korai Paratethys története. Földtani Közlöny, 110, 456-472.

Basch, O., Pavelić, D. and Bakrač, K. (1995): Gornjopontski facijesi sjevernog krila Konjšćinske sinklinale kod Huma Zabočkog (Hrvatsko Zagorje). In: Vlahović, I., Velić, I. and Šparica, M. (Eds.): First Croatian geological congress, Proceedings. Institute of Geology, Croatian Geological Society, Zagreb, 57-61.

Bjørlykke, K. and Egeberg, P.K. (1993): Quartz cementation in sedimentary basins. American Association of Petroleum Geologists Bulletin, 77, 1536-1548.

Burley, S.D., Kantorwicz, J.D. and Waugh, B. (1985): Clastic diagenesis. In: Brenchley, P. and Williams, B.P.B. (Eds.): Sedimentology: Recent and Applied Aspects. Spec. Publ. Geol. Soc. London, 18, 189-226. Blackwell Scientific Publications, Oxford.

Curtis, C.D. (1977): Sedimentary geochemistry: environments and processes dominated by involvement of an aqueous phase. Philosophical Transactions of the Royal Society, London, 286, 353-372.

Curtis, C.D. (1983): Geochemistry of porosity enhancement and reduction on clastic sediments. In: Brooks, J. (Ed.): Petroleum Geochemistry and Exploration of Europe. Spec. Publ. Geol. Soc. London, 12, 113-125. Blackwell Scinetific Publications, Oxford.

Cvetković, M., Emanović, I., Stopar, A. and Slavinić, P. (2018): Petroleum system modeling and assessment of the remaining hydrocarbon potential in the eastern part of Drava Depression. Interpretation, 6, 1, SB11-SB21.

Cvetković, M., Matoš, B., Rukavina, D., Kolenković Močilac, I., Saftić, B., Baketarić, T., Baketarić, M., Vuić, I., Stopar, A., Jarić, A. and Paškov, T. (2019) Geoenergy potential of the Croatian part of Pannonian Basin: insights from the reconstruction of the pre-Neogene basement unconformity. Journal of Maps, 15 (2), 651–661.

de Caritat, P. and Baker, J.C. (1992): Oxygen isotope evidence for upward cross formational flow in a sedimentary basin near maximum burial. Sedimentary Geology, 78, 155-164.

Dolton, L.G. (2006): Pannonian Basin Province, Central Europe (Province 4808) – Petroleum geology, total petroleum systems, and petroleum resource assessment. U.S. Geological Survey, Bulletin 2204-B. doi: 10.3133/b2204B

Ehrenberg, S.N. (1993): Preservation of anomalously high porosity in deeply buried sandstones by grain coating chlorite: Example from the Norwegian continental shelf. American Association of Petroleum Geologists Bulletin, 77, 1260-1286.

Ehrenberg, S.N. and Jakobsen, K.G. (2001): Plagioclase dissolution related to biodegradation of oil in Brent Group sandstones (Middle Jurassic) of Gullfaks Field, northern North Sea. Sedimentology, 48, 703-722.

Elmore, R.D., Engel, M.H., Crawford, L., Nick, K., Imbus, S. and Sofer, Z. (1987): Evidence for a relationship between hydrocarbon migration and authigenic magnetite. Nature, 325, 428-430.

Giles, M.R. and de Boer, R.B. (1990): Origin and significance of redistributional secondary porosity. Marine and Petroleum Geology, 7, 378-397.

Griffiths, J., Worden, R.H., Wooldridge, L.J., Utley, J.E.P., Duller, R.A. and Edge, R.L. (2019) Estuarine clay mineral distribution: Modern analogue for ancient sandstone reservoir quality prediction. Sedimentology, 66, 2011–2047.

Grizelj, A., Tibljaš, D., Kovačić, M. and Španić, D. (2011) Diagenesis of Miocene pelitic sedimentary rocks in the Sava Depression (Croatia). Clay Minerals, 46 (1), 59–72.

Grizelj, A., Milošević, M., Bakrač, K., Galović, I., Kurečić, T., Hajek-Tadesse, V., Avanić, R., Miknić, M., Horvat, M., Čaić, A. and Matošević, M. (2020): Paleoecological and sedimentological characterization of Middle Miocene sediments from the Hrvatska Kostajnica area (Croatia). Geologia Croatica, 73, 3, 153-175. https://doi.org/10.4154/gc2020.15

Grizelj, A., Milošević, M., Miknić, M., Hajek-Tadesse, V., Bakrač, K., Galović, I., Badurina, L., Kurečić, T., Wacha, L., Šegvić, B., Matošević, M., Čaić-Janković, A. and Avanić, R. (2023): Evidence of Early Sarmatian volcanism in the Hrvatsko Zagorje Basin, Croatia – mineralogical, geochemical and biostratigraphic approaches. Geologica Carpathica, 74, 1, 59-82. https://doi.org/10.31577/GeolCarp.2023.02

Harzhauser, M., Latal, C. and Piller, W. (2007): The stable isotope archive of Lake Pannon as a mirror of Late Miocene climate change. Palaeogeography, Palaeoclimatology, Palaeoecology, 249, 335-350. doi: 10.1016/j.palaeo.2007.02.006

Harzhauser, M. and Piller, W.E. (2007): Benchmark data of a changing sea – palaeogeography, palaeobiogeography and events in the Central Paratethys during the Miocene. Palaeogeography, Palaeoclimatology, Palaeoecology, 253, 8–31. doi: 10.1016/j.palaeo.2007.03.031

Harzhauser, M. and Mandic, M. (2008): Neogene lake systems of the Central and South-Eastern Europe – faunal diversity, gradients and interrelations. Palaeogeography, Palaeoclimatology, Palaeoecology, 260, 417-434. doi: 10.1016/j.palaeo.2007.12.013

Hermanns Stengele, R. and Plötze, M. (2000): Suitability of minerals for controlled landfill and containment. In: Vaughan, D.J. and Wogelius, R.A. (Eds.): Environmental Mineralogy. European Mineralogical Union Notes in Mineralogy, 2, Eötvös University Press, Budapest, 291-331.

Hilgen, F.J., Lourens, L.J. and van Dam, J.A. (2012): The Neogene Period. In: Gradstein, F.M., Ogg, J.G., Schmitz, M. and Ogg, G. (Eds.): The Geological Time scale 2012. Elsevier, Amsterdam, 923-978.

Horváth, F., Musitz, B., Balázs, A., Vegh, A., Uhrin, A., Nador, A., Koroknai, B., Pap, N., Toth, T. and Worum, G. (2015): Evolution of the Pannonian basin and its geothermal resources. Geothermics, 53, 328–352. doi: 10.1016/j.geothermics.2014.07.009

Hurst, A.R. (1987): Problem of reservoir characterization in some North Sea sandstone reservoirs solved by the application of microscale geological data. In: Kleppe, J., Berg, E.W., Buller, A.T., Hjelmeland, O. and Torsaeter, O. (Eds.): North Sea Oil and Gas Reservoirs, 153-167. Norwegian Petroleum Directorate, Graham and Trotman, London.

Ivković, Ž., Matej, S. and Škoko, M. (2000): Seismostratigraphic interpretation of Upper Miocene and Pliocene sediments of the Sava depression. In: Vlahović I. and Biondić R. (Eds.): Second Croatian Geological Congress, Proceedings, Zagreb, 219-222.

Jackson, S.A. and Beales, F.W. (1967): An aspect of sedimentary basin evolution: The concentration of Mississippi-Valley type ores during the late stages of diagenesis. Canadian Petroleum Geology Bulletin, 15, 383-433.

Juhász, GY. (1994): Comparison of the sedimentary sequences in Late Neogene subbasins in the Pannonian Basin, Hungary (Magyarországi neogén medencerészek pannóniai s.l. üledéksorának összehasonlító elemzése). Földtani Közlöny, 124, 4, 341–365.

Kantorowicz, J.D., Eigner, M.R.P., Livera, S., van Schijndel-Goester, F.S. and Hamilton, P.J. (1992): Integration of petroleum engineering studies of producing Brent Group fields to predict reservoir properties in the Pelican Field, UK North Sea. In: Morton, A.C., Haszeldine, R.S., Giles, M.R. and Brown, S. (Eds.): Geology of the Brent Group. Spec. Publ. Geol. Soc. London, 61, 453-469.

Kolenković, I., Saftić, B. and Perešin, D. (2013): Regional capacity estimates for CO2 geological storage in deep saline aquifers – Upper Miocene sandstones in the SW part of the Pannonian basin. InternationalJournal of Greenhouse Gas Control, 16, 180-186.

Kolenković Močilac, I., Cvetković, M., Saftić, B. and Rukavina, D. (2022): Porosity and permeability model of a regional extending unit (Upper Miocene sandstones of the western part of Sava Depression, Croatia) based on vintage well data. Energies, 15, 6066. doi: 10.3390/en15166066

Kováč, M., Márton, E., Oszczypko, N., Vojtko, R., Hók, J., Králiková, S., Plašienka, D., Klučiar, T., Hudáčková, N. and Oszczypko-Clowes, M. (2017): Neogene palaeogeography and basin evolution of the Western Carpathians, Northern Pannonian domain and adjoining areas. Global and Planetary Change, 155, 133-154. doi: 10.1016/j.gloplacha.2017.07.004

Kováč, M., Halásová, E., Hudáčková, N., Holcová, K., Hyžný, M., Jamrich, M. and Ruman, A. (2018): Towards better

correlation of the Central Paratethys regional time scale with the standard geological time scale of the Miocene Epoch. Geologica Carpathica, 69, 3, 283–300. doi: 10.1515/geoca-2018-0017

Kovačić, M., Zupanič, J., Babić, L., Vrsaljko, D., Miknić, M., Bakrač, K., Hećimović, I., Avanić, R. and Brkić, M. (2004): Lacustrine basin to delta evolution in the Zagorje Basin, a Pannonian sub-basin (Late Miocene: Pontian, NW Croatia). Facies, 50/1, 19-33.

Kovačić, M. and Grizelj, A. (2006): Provenance of the Upper Miocene clastic material in the southwestern Pannonian Basin. Geologica Carpathica, 57, 495-510.

Kurečić, T., Kovačić, M. and Grizelj, A. (2021): Mineral assemblage and provenance of the Pliocene Viviparus beds from the area of Vukomeričke Gorice (Central Croatia). Geologia Croatica 74 (3), 253-271. https://doi.org/10.4154/gc.2021.16

Liu, Z., Colin, C., Huang, W., Chen, Z., Trentesaux, A. and Chen, J. (2007) Clay minerals in surface sediments of the Pearl River drainage basin and their contribution to the South China Sea. Chinese Science Bulletin, 52 (8), 1101-1111.

Love, L.G. (1967): Early diagenetic iron sulphide in recent sediments of Wash (England). Sedimentology, 9, 327-352.

Lučić, D., Saftić, B., Krizmanić, K., Prelogović, E., Britvić, V., Mesić, I. and Tadej, J. (2001): The Neogene evolution and hydrocarbon potential of the Pannonian Basin in Croatia. Marine and Petroleum Geology, 18, 133-147. doi: 10.1016/S0264-8172(00)00038-6

Macenić, M., Kurevija, T. and Medved, I. (2020): Novel geothermal gradient map of the Croatian part of the Pannonian Basin System based on data interpretation from 154 deep exploration wells. Renewable and Sustainable Energy Reviews, 132, 110069. doi: 10.1016/j.rser.2020.110069

Magyar, I., Geary, D.H. and Müller, P. (1999): Palaeogeographic evolution of the Late Miocene Lake Pannon in central Europe. Palaeogeography, Palaeoclimatology, Palaeoecology, 147, 151-167. doi: 10.1016/S0031-0182(98)00155-2

Magyar, I., Radivojević, D., Sztanó, O., Synak, R., Ujszászi, K. and Pócsik, M. (2013): Progradation of the Palaeo-Danube shelf margin across the Pannonian Basin during the Late Miocene and Early Pliocene. Global and Planetary Change, 103, 168-173. doi: 10.1016/j.gloplacha.2012.06.007

Magyar, I. (2021): Chronostratigraphy of clinothem-filled non-marine basins: Dating the Pannonian Stage. Global and Planetary Change, 205, 103609. doi: 10.1016/j.gloplacha.2021.103609

Malvić, T. and Velić, J. (2011): Neogene tectonics in Croatian part of the Pannonian Basin and reflectance in hydrocarbon accumulations. In: Schattner, U. (Ed.): New frontiers in tectonic research: At the midst of plate convergence. – Intech, Rijeka, 215-238.

Mandic, O., Kurečić, T., Neubauer, T.A. and Harzhauser, M. (2015): Stratigraphic and palaeogeographic significance of lacustrine molluscs from the Pliocene Viviparus beds in Central Croatia. Geologia Croatica, 68, 179–207. doi: 10.4154/GC.2015.15

Matenco, L. and Radivojević, D. (2012): On the formation and evolution of the Pannonian Basin: Constraints derived from the structure of the junction area between the Carpathians and Dinarides. Tectonics, 31, 6, TC6007. https://dx.doi.org/10.1029/2012TC003206

Matošević, M., Slavković, R. and Tomašić, N. (2015): Occurrence of radiating Fe-oxides and Fe-oxyhydroxides crystal groups in the rocks of cores from the borehole Bunjani-59, Croatia. In: Ambriović Ristov, A., Gajović, A., Weber, I. and Vidoš, A. (Eds.): Proceedings of the 3rd Croatian Microscopy Congress with International Participation, Zadar, Croatia, April 26-29, 2015. Ruđer Bošković Institute and Croatian Microscopy Society, 83-84.

Matošević, M. and Šuica, S. (2017): Microstructural characteristics of staurolite from mica schist of the Drava depression basement (Croatia). In: Gajović, A., Weber, I., Kovačević, G., Čadež, V., Šegota, S., Peharec Štefanić, P. and Vidoš, A. (Eds.): 13th Multinational Congress on Microscopy: Book of abstracts, Rovinj, Croatia, September 24-29, 2017. Ruđer Bošković Institute and Croatian Microscopy Society, 520-521.

Matošević, M., Krizmanić, K., Zlatar, S., Hernitz Kučenjak, M., Mikša, G. and Pecimotika, G. (2019a): Using ultraviolet light for fast sedimentological analysis and characterization of reservoir rocks: A case study of the Upper Miocene sediments from the Sava Depression, Croatia. Proceedings of the 34th IAS Meeting of Sedimentology. Rome, Italy, September 10-13, 2019. The International Association of Sedimentologists and the Earth Science Department of Sapienza University of Roma

Matošević, M., Pavelić, D. and Kovačić, M. (2019b): Petrography of the Upper Miocene sandstones from the Sava and Drava Depressions: Basis for understanding the provenance and diagenesis of the largest hydrocarbon reservoirs in the North Croatian Basin. In: Horvat, M., Matoš, B. & Wacha, L. (Eds.): Proceedings of the 6th Croatian Geological Congress with International Participation. Zagreb, Croatia, October 9-12, 2019. Croatian Geological Society, 127-128.

Matošević, M., Hernitz Kučenjak, M., Premec Fućek, V., Krizmanić, K., Mikša, G. and Troskot-Čorbić, T. (2019c): The middle Badenian deep-marine sedimentation in the Central Paratethys: A case study of the Sava depression in the North Croatian Basin. In: Horvat, M., Matoš, B. & Wacha L. (Eds.): Proceedings of the 6th Croatian Geological Congress with International Participation. Zagreb, Croatia, October 9-12, 2019. Croatian Geological Society, 128-129.

Matošević, M., Kovačić, M. and Pavelić, D. (2021): Provenance and diagenesis of the Upper Miocene sandstones from the Pannonian Basin System. In: Bábek, O. and Vodrážková, S. (Eds.): Book of Abstract of the 35th IAS Meeting of Sedimentology, Virtual Meeting. Prague, Czech Republic, June 21-25, 2021. Olomouc 2021, 300.

Matošević, M., Marković, F., Bigunac, D., Šuica, S., Krizmanić, K., Perković, A., Kovačić, M. and Pavelić, D. (2023a): Petrography of the Upper Miocene sandstones from the North Croatian Basin: Understanding the genesis of the largest reservoirs in the southwestern part of the Pannonian Basin System. Geologica Carpathica, 74/2, 155-179. doi: 10.31577/GeolCarp.2023.06

Matošević, M., Šuica, S., Wall, C.J.,Mužina, M., Vranjković, A., Zopf, D. and Jović, G. (2023b): The oldest Miocene volcaniclastics of the Carpathian–Pannonian Region based on U–Pb zircon LA-ICP-MS dating in the Mura Depression (Northwestern Croatia). In: Vlahović, I. and Matešić, D. (Eds.): Abstracts Book of the 36th International Meeting of Sedimentology. Dubrovnik, Croatia, June 12-16, 2023. Croatian Geological Society, 318.

Matošević, M., Garzanti, E., Šuica, S., Bersani, D., Marković, F., Razum, I., Grizelj, A., Petrinjak, K., Kovačić, M. and Pavelić, D. (2024): The Alps as the main source of sand to the Late Miocene Lake Pannon (Pannonian Basin, Croatia). Geologia Croatica, 77 (2), 13-27.

Moore, D.M. and Reynolds, R.C. (1997): X-ray Diffraction and the Identification and Analysis of Clay Minerals, 2nd Edition, Oxford University Press, New York.

Morad, S., Marfil, R. and de la Pena, J.A. (1989): Diagenetic K-feldspar pseudomorphs in the Triassic Buntsandstein sandstones of the Iberian Range, Spain. Sedimentology, 36, 635-650.

Morad, S. (1998): Carbonate cementation in sandstones. Spec. Publs Int. Assoc. Sediment., 26, 511 pp. Blackwell Science, Oxford.

Morad, S., Ketzer, J.M. and de Ros, L.F. (2000): Spatial and temporal distribution of diagenetic alterations in siliciclastic rocks: implications for mass transfer in sedimentary basins. Sedimentology, 47 (Millenium Reviews), 95-120.

Neasham, J.W. (1977): Applications of scanning electron microscopy to characterization of hydrocarbon-bearing rocks: Scanning Electron Microscopy, 10, 101-108.

Pamić, J. (1999): Kristalinska podloga južnih dijelova Panonskog bazena – temeljena na površinskim i bušotinskim podacima. Nafta, 50/9, 291-310.

Panalytical, 2004. X'Pert High Score Plus, version 2.1. Panalytical, Almelo, The Netherlands.

Pavelić, D. (2001): Tectonostratigraphic model for the North Croatian and North Bosnian sector of the Miocene Pannonian Basin System. Basin Research, 13, 359–376. doi: 10.1046/j.0950-091x.2001.00155.x

Pavelić, D. and Kovačić, M. (2018): Sedimentology and stratigraphy of the Neogene rift-type North Croatian Basin (Pannonian Basin System, Croatia): A review. Marine and Petroleum Geology, 91, 455-469. doi: 10.1016/j.marpetgeo.2018.01.026

Piller, W., Harzhauser, M. and Mandic, O. (2007): Miocene Central Paratethys stratigraphy – current status and future directions. Stratigraphy, 4, 151–168. doi: 10.29041/strat.04.2.09

Pittman, E.D. and King, G.E. (1986): Petrology and formation damage control, Upper Cretaceous sandstone, offshore Gabon. Clay minerals, 21, 7781-790.

Pittman, E.D. and Larese, R.E. (1991): Compaction of lithic sands: experimental results and application. American Association of Petroleum Geologists Bulletin, 75, 1279-1299.

Podbojec, M. and Cvetković, M. (2016): Preliminary estimate of CO2 storage capacity by petrophysical modelling in Upper Miocene Poljana Sandstones in the western part of the Sava Depression. Rudarsko-geološko-naftni zbornik, 31, 1, 31-43.

Pogácsás GY. 1984: Seismic stratigraphic features of the Neogene sediments in the Pannonian Basin. Geofizikai Közlemények 30 (4), 373–410.

Premec Fućek, V., Galović, I., Mikša, G., Hernitz Kučenjak, M., Krizmanić, K., Hajek-Tadesse, V., Matošević, M., Pecimotika, G. and Zlatar, S. (2022): Paleontological and lithological evidence of the late Karpatian to early Badenian marine succession from Medvednica Mountain (Croatia), Central Paratethys. International Journal of Earth Sciences. https://doi.org/10.1007/s00531-022-02264-4

Robin, P.-Y.F. (1978): Pressure solution at grain-to-grain contacts. Geochimica Cosmochimica Acta, 42, 1383-1389.

Rögl, F. and Steininger, F.F. (1983): Vom Zerfall der Tethys zu Mediterran und Paratethys. Die Neogene Palaeogeographie und Palinspastik des zirkum-mediterranen Raumes. Annalen des Naturhistorischen Museum in Wien, 85 A, 135-163.

Rögl, F. (1998): Palaeogeographic considerations for Mediterranean and Paratethys seaways (Oligocene to Miocene). Annalen des Naturhistorischen Museum in Wien, 99 A, 279-310.

Royden, L.H. (1988): Late cenozoic tectonics of the Pannonian Basin System. In: Royden, L.H. and Horváth, F. (Eds.): The Pannonian Basin: A Study in Basin Evolution. AAPG Memoir, 45, 27–48. doi: 10.1306/M45474C3

Rukavina, D., Saftić, B., Matoš, B., Kolenković Močilac, I., Premec Fućek, V. and Cvetković, M. (2023): Tectonostratigraphic analysis of the syn-rift infill in the Drvaa Basin, southwestern Pannonian Basin System. Marine and Petroleum Geology, 152, 106235. doi: 10.1016/j.marpetgeo.2023.106235

Saftić, B., Velić, J., Sztanó, O., Juhász, GY. and Ivković, Ž. (2003): Tertiary subsurface facies, source rocks and hydrocarbon reservoirs in the SW part of the Pannonian Basin (northern Croatia and south-western Hungary). Geologia Croatica, 56, 101-122.

Schmidt, V. and McDonald, D.A. (1979): The role of secondary porosity in the course of sandstone diagenesis. In: Scholle, P.A. and Schuldger, P.R. (Eds.): Aspects of Diagenesis. Soc. Econ. Paleont. Miner. Spec. Publ., Tulsa, OK, 29, 175-207.

Šćavničar, B. (1979) Sandstones of the Pliocene and Miocene age in the Sava River depression. Znan savjet za naftu Jugosl akad znan umjet. 3rd Znan Skup Sekc Primj Geol Geof Geokem 2:351–382.

Sebe, K., Kovačić, M., Magyar, I., Krizmanić, K., Špelić, M., Bigunac, D., Sütő-Szentai, M., Kovács, Á., Szuromi-Korecz, A., Bakrač, K., Hajek-Tadesse, V., Troskot-Čorbić, T. and Sztanó, O. (2020): Correlation of upper Miocene-Pliocene Lake Pannon deposits across the Drava Basin, Croatia and Hungary. Geologia Croatica, 73, 3, 177-195. doi: 10.4154/gc.2020.12

Severin, K.P. (2004): Energy dispersive spectrometry of common rock forming minerals. Dordrecht, The Netherlands. Kluwer Academic Publishers. https://doi.org/10.1007/978-1-4020-2841-0

Sneider, R.M. (1990): Reservoir Description of Sandstones. In: Barwis, J.H., Mcpherson, J.G. and Studlick, J.R.J. (Eds.): Sandstone Petroleum Reservoirs. – Casebooks in

Earth Sciences. Springer, New York, 1-3. doi: 10.1007/978-1-4613-8988-0_1

Špelić, M., Sztanó, O., Saftić, B. and Bakrač K. (2019): Sedimentary basin fill of Lake Pannon in the eastern part of Drava. In: Horvat, M., Matoš, B. and Wacha, L. (Eds.): Proceedings of the 6th Croatian Geological Congress with international participation. Zagreb, October 9-12, 2019, Croatian Geological Society, 192-193.

Špelić, M., Kovács, Á., Saftić, B. and Sztanó, O. (2023): Competition of deltaic feeder systems reflected by slope progradation: a high-resolution example from the Late Miocene-Pliocene, Drava Basin, Croatia. International Journal of Earth Sciences, 112, 1023–1041. doi: 10.1007/s00531-023-02290-w

Steininger, F.F. and Rögl, F. (1979): The Paratethys history - a contribution towards the Neogene geodynamics of the Alpine Orogene (an abstract). Ann. Géol. Pays Hellén., Tome hors serie, fasc. III, 1153-1165, Athens.

Šuica, S., Garašić, V. and Woodland, A.B. (2022a): Petrography and geochemistry of granitoids and related rocks from the pre-Neogene basement of the Slavonia–Srijem Depression (Croatia). Geologia Croatica, 75, 129–144. doi: 10.4154/gc.2022.09

Šuica, S., Tapster, S.R., Mišur, I. and Trinajstić, N. (2022b): The Late Cretaceous syenite from the Sava suture zone (eastern Croatia). In: XXII International Congress of the CBGA, Plovdiv, Bulgaria, 7-11 September 2022, Abstracts, 100.

Sztanó, O., Szafián, P., Magyar, I., Horányi, A., Bada, G., Hughes, D.W., Hoyer, D.L. and Wallis, R.J. (2013): Aggradation and progradation controlled clinothems and deep-water sand delivery model in the Neogene Lake Pannon, Makó Trough, Pannonian Basin, SE Hungary. Global and Planetary Change, 103, 149–167. doi: 10.1016/j.gloplacha.2012.05.026

Sztanó, O., Sebe, K., Csillag, G. and Magyar, I. (2015): Turbidites as indicators of Palaeotopography, Upper Miocene Lake Pannon, Western Mecsek Mountains (Hungary). Geologica Carpathica, 66, 331-344. doi: 10.1515/geoca-2015-0029

Tadej, J., Marić Đureković, Ž. and Slavković, R. (1996): Porosity, Cementation, Diagenesis and Their Influence on the Productive Capability of Sandstone Reserevoirs in the Sava Depression (Croatia). Geologia Croatica, 49, 311-316.

Tari, G., Horváth, F. and Rumpler, J. (1992): Styles of extension in the Pannonian Basin. Tectonophysics, 208, 203–219. https://doi.org/10.1016/0040-1951(92)90345-7

Taylor, J.M. (1950): Pore space reduction in sandstones. American Association of Petroleum Geologists Bulletin, 34, 701-716.

Ter Borgh, M., Vasiliev, I., Stoica, M., Knežević, S., Matenco, L., Krijgsman, W., Rundić, LJ. and Cloetingh, S. (2013): The isolation of the Pannonian basin (Central Paratethys): New constrains from magnetostratigraphy and biostratigraphy. Global and Planetary Change, 103, 99-118. doi: 10.1016/j.gloplacha.2012.10.001

Tiab, D. and Donaldson, C.E. (2004): Petrophysics: Theory and Practice of Measuring Reservoir Rock and Fluid Transport Properties. 2nd edition, Gulf Professional Publishing, Elsevier, Inc., Oxford.

Tuschl, M., Kurevija, T., Krpan, M. and Macenić, M. (2022): Overview of the current activities related to deep geothermal energy utilisation in the Republic of Croatia. Clean Technologies and Environmental Policy, 24, 3003–3031. doi: 10.1007/s10098-022-02383-1

Velić, J., Malvić, T., Cvetković, M. and Vrbanac, B. (2012): Reservoir geology, hydrocarbon reserves and production in the Croatian part of the Pannonian Basin System. Geologia Croatica, 65, 91-101. doi: 10.4154/GC.2012.07

Vrbanac, B., Velić, J. and Malvić, T. (2010): Sedimentation of deep-water turbidites in the SW part of the Pannonian Basin. Geologica Carpathica, 61, 1, 55-69. doi: 10.2478/v10096-010-0001-8

Vulin, D., Kolenković Močilac, I., Jukić, L., Arnaut, M., Vodopić, F., Saftić, B., Karasalihović Sedlar, D. and Cvetković, M. (2023): Development of CCUS clusters in Croatia. International Journal of Greenhouse Gas Control, 124, 103857.

Waugh, B. (1971): Formation of quartz overgrowths in the Penrith Sandstone (Lower Permian) of northwest England as revealed by scanning electron microscopy. Sedimentology, 17, 309-320.

Welton, J.E. (1984): SEM Petrology Atlas. AAPG, Tusla, Oklahoma, USA, 237 p.

Wentworth C.K. (1922): A scale of grade and class terms for clastic sediments. The Journal of Geology, 30, 5, 377-392.

Warren, E.A. and Curtis, C.D. (1989): The chemical composition of authigenic illite within two sandstone reservoirs as analysed by ATEM. Clay Minerals, 24, 137-156.

Worden, R.H., Mayall, M.J. and Evans, I.J. (1997): Predicting reservoir quality during exploration: lithic grains, porosity and permeability in Tertiary clastic rocks of the South China Sea Basin. Geological Society of London, Special Publications, 126, 107-115. doi: 10.1144/GSL.SP.1997.126.01.08

Worden, R.H., Coleman, M.L. and Matray, J.M. (1999): Basin scale evolution of formation waters: a diagenetic and formation water study of the Triassic Chaunoy Formation, Paris Basin. Geochimica et Cosmochimica Acta, 63, 2512-2528.

Worden, R.H., Mayall, M.J. and Evans, I.J. (2000): The effect of ductile-lithic sand grains and quartz cement on porosity and permeability in Oligocene and Lower Miocene clastics, South China Sea: predictionof reservoir quality. American Association of Petroelum Geologists Bulletin, 84, 345-359.

Worden, R.H. and Morad, S. (2000): Quartz Cementation in Sandstones. Spec. Publs. Int. Assoc. Sediment., 29, 342, Blackwell Science, Oxford.

Worden, R.H. and Burley, S.D. (2003): Sandstone diagenesis: the evolution of sand to stone. In: Burley, S.D and Worden, R.H. (Eds.): Sandstone Diagenesis: Recent and Ancient. International Association of Sedimentologists, 4, 3-44.

APPENDIX

SUPPORTING INFORMATION

Supporting Information is hosted online at https://hrcak.srce.hr/ojs/index.php/rgn/article/view/30841

SAŽETAK

Procjena kvalitete ležišta: Otkrivanje dijagenetskih promjena mineraloškim i petrofizičkim analizama gornjomiocenskih jezerskih pješčenjaka u Panonskome bazenskom sustavu, Hrvatska

Gornjomiocenski jezerski pješčenjaci Sjevernohrvatskoga bazena, smještenoga u jugozapadnome dijelu Panonskoga bazenskog sustava, čine važna ležišta ugljikovodika, no razvoj njihovih dijagenetskih procesa još uvijek nije dovoljno istražen. Ovo istraživanje nudi sveobuhvatan pregled dijageneze tih pješčenjaka analizirajući uzorke iz istražnih bušotina u Savskoj i Dravskoj depresiji. Koristeći se petrografskim analizama, skenirajućom elektronskom mikroskopijom s energijski disperzivnom rendgenskom spektroskopijom (SEM-EDS), rendgenskom difrakcijom (XRD) i petrofizičkim mjerenjima, cilj istraživanja bio je objasniti dijagenetske procese koji utječu na kvalitetu ležišta nafte i plina i njihovu produktivnost. Rezultati otkrivaju konzistentnu distribuciju veličine zrna, modalnoga sastava i dijagenetskih promjena pješčenjaka u objema depresijama. Kompakcija, koja se očituje kroz razvoj zrnskih kontakata i tlačno otapanje, dovodi do smanjenja poroznosti s dubinom. Karbonatni cementi, osobito kalcit i Fe-dolomit/ankerit, glavni su čimbenici smanjenja primarne međuzrnske poroznosti, uz minerale glina, kvarc, feldspate itd. Sekundarna poroznost rezultat je otapanja minerala i procesa redistribucije koji također znatno utječu na cjelokupan razvoj poroznosti. Minerali glina, detritalni i autigeni, pokazuju kompleksno međudjelovanje s drugim dijagenetskim procesima, dodatno utječući na smanjenje poroznosti i propusnosti. Autigeni minerali glina, uključujući ilit, klorit i kaolinit, djeluju kao cementi koji ispunjavaju pore ili se javljaju u vidu prevlaka na zrnima, sprečavajući dodatno protok fluida. Paragenetski procesi ocrtavaju složeni odnos između mineraloških transformacija i petrofizičkih svojstava definirajući kvalitetu ležišta. Razumijevanje dinamike dijagenetskih procesa ključno je za predviđanje kvalitete ležišta, putove migracija fluida i ugljikovodičnu produktivnost. Ovo istraživanje popunjava bitnu prazninu u znanju o dijagenezi gornjomiocenskih jezerskih pješčenjaka u jugozapadnome dijelu Panonskoga bazena, pružajući uvide važne za energetski sektor i podržavajući održivi razvoj resursa u regiji.

Ključne riječi:
pješčenjački rezervoari, dijageneza, poroznost, Sjevernohrvatski bazen, kasni miocen

Author's contribution

Mario Matošević (1) (PhD student at the Faculty of Mining, Geology and Petroleum Engineering, University of Zagreb, and Geology Expert at INA – Industrija nafte d.d.) provided sample collection, sample preparation, petrographic, mineralogical, and SEM-EDS analyses, data interpretation, interpretation of petrophysical results, conceptualization and drafting of the article, and graphical representations. **Nenad Tomašić, PhD (2)** (Full Professor at the Faculty of Science, University of Zagreb) provided sample preparation, XRD analyses, data interpretation, interpretation of XRD results and comparison with petrophysical data. **Adaleta Perković (3)** (PhD and Core Analyses Expert at INA – Industrija nafte d.d.) provided sample preparation, petrophysical (porosity) measurements, data interpretation, interpretation of petrophysical results and comparison with mineralogical data, and graphical representations. **Štefica Kampić (4)** (Expert at the Faculty of Science, University of Zagreb) provided sample preparation and assistance with XRD analyses. **Marijan Kovačić, PhD (5)** (Full Professor at the Faculty of Science, University of Zagreb) provided conceptualization and drafting of the article, data interpretation, interpretation of mineralogical results, and contributing with geology of the Neogene North Croatian Basin. **Davor Pavelić, PhD (6)** (Full Professor at the Faculty of Mining, Geology and Petroleum Engineering, University of Zagreb) provided conceptualization and drafting of the article, data interpretation, and contributing with geology of the Neogene North Croatian Basin.